Title
SUPERCONDUCTING COMPONENTS FOR INFRARED AND MILLIMETER WAVE RECEIVERS

Authors
Richards, P.L.
Hu, Q.

Publication Date
1988-10-01

LBL-26169
Preprint

Center for Advanced Materials

CAM

Submitted to Proceedings of the IEEE

Superconducting Components for Infrared and Millimeter Wave Receivers

P.L. Richards and Q. Hu

October 1988

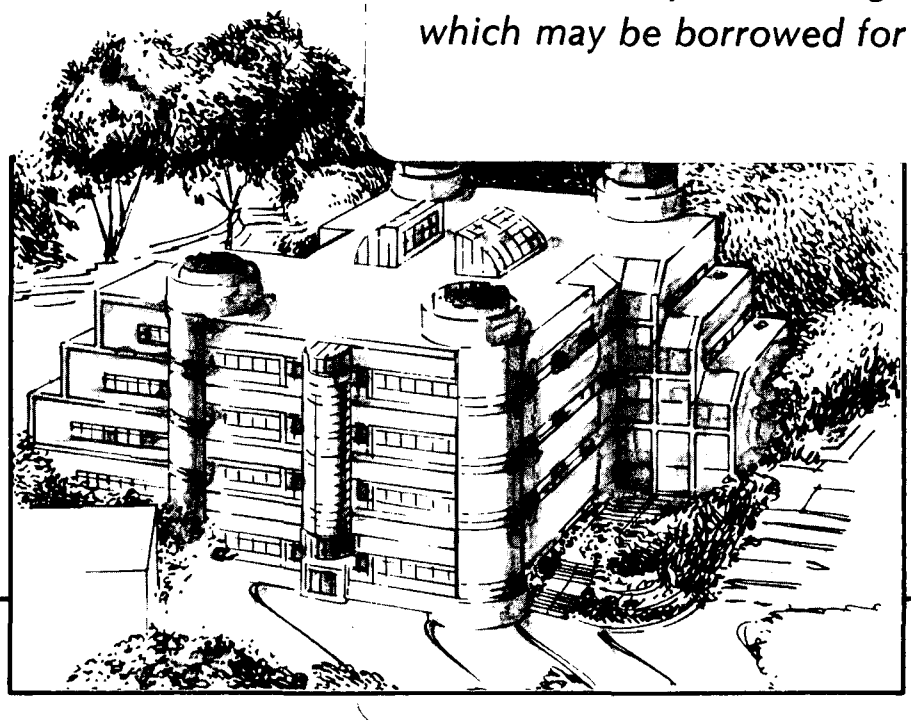

Materials and Chemical Sciences Division

Lawrence Berkeley Laboratory • University of California

ONE CYCLOTRON ROAD, BERKELEY, CA 94720 • (415) 486-4755

Prepared for the U.S. Department of Energy under Contract DE-AC03-76SF00098

DISCLAIMER

LBL-26169

SUPERCONDUCTING COMPONENTS FOR INFRARED AND MILLIMETER WAVE RECEIVERS

P.L. Richards and Qing Hu

Department of Physics, University of California and

Center for Advanced Materials, Materials and Molecular

Research Division, Lawrence Berkeley Laboratory,

1 Cyclotron Road, Berkeley, California 94720, USA

Abstract--A review is given of the superconducting components that have been developed for infrared and millimeter wave receivers. A brief description is given of the scientific principles on which each device is based, followed by a discussion of the performance that has been achieved in terms of the appropriate figures of merit. Finally, comments are made about the possibility that useful device performance can be achieved by using the new high T_c oxide superconductors. This review emphasizes photon-assisted quasiparticle tunneling and the SIS quasiparticle mixer, which is the only superconducting component to find substantial applications at infrared or millimeter wavelengths. Descriptions are given of the SIS quasiparticle direct detector, the Josephson effect oscillator, the Josephson effect parametric amplifier and the various superconducting bolometers, for which practical applications appear possible. The less promising Josephson effect detector and mixer and also the various ideas for superconducting photon detectors are described because of the current interest in possible high T_c versions of these devices.

I. INTRODUCTION

The earliest superconducting device for infrared or millimeter waves was a bolometric infrared detector that uses the temperature dependent resistance of a superconducting film at the critical temperature T_c as the thermometer. Later, the discovery of Josephson tunneling led to a spectacular flow of ideas about detectors, mixers, oscillators, and parametric amplifiers. After the limitations of the Josephson detectors and mixers became clear, the device possibilities of the quasiparticle tunneling currents were explored and the SIS quasiparticle detector and mixer were developed. As is usual with device development, only a few of the devices that have been investigated have the potential for doing some important task better than competing technologies.

In this review, emphasis will be given to the SIS quasiparticle heterodyne mixer, which is the only superconducting infrared or millimeter wave device which has had significant practical applications. Less emphasis will be given to other devices such as the SIS quasiparticle direct detector, the Josephson effect oscillator, the Josephson effect parametric amplifier and the various superconducting bolometers for which practical applications appear possible. In addition, a few of the less promising devices will be described.

The discovery of high T_c superconductors has stimulated investigations of both old and new superconducting devices for infrared and millimeter waves. Comments will be made wherever possible about the impact of the new high T_c materials on the prospects for all of the devices discussed. The high T_c transition edge bolometer appears to be useful in its present form. If the required junctions can be made from high T_c materials, quasiparticle and Josephson devices can be operated well above LHe temperatures, but usually with

significant degradation in important figures of merit. If very low capacitance and very high current density junctions can be made, high T_c quasiparticle and Josephson devices can be operated at much higher frequencies than can be done with conventional superconductors.

Frequent reference will be made throughout this review to well known properties and figures of merit for infrared and millimeter wave devices. Direct detectors are characterized in terms of the dark current or the detector noise limit to the noise equivalent power (NEP), the responsivity S, and the dynamic range, or saturation power P_{sat}. Heterodyne receivers are described by the mixer noise temperature T_M, the mixer gain G, the IF amplifier noise temperature T_{IF}, the receiver noise temperature $T_R=T_M+T_{IF}/G$, and the saturation power P_{sat}. Receivers based on direct detectors are used for broad bandwidths and high frequencies. Coherent receivers which use heterodyne mixers and parametric preamplifiers are used for narrow bandwidths and low frequencies. The crossover between these approaches is at ~300 GHz for a fractional bandwidth of 10^{-1} and ~2 THz for a fractional bandwidth of 10^{-5}. Coherent amplifiers and mixers, as well as direct detectors that are coupled to the electromagnetic field by an antenna, are sensitive to only one electromagnetic mode with throughput $A\Omega=\lambda^2$. Here A is the area of the focal spot and Ω the solid angle of the focus. Other detectors, such as the superconducting bolometer have a sensitive area of arbitrary size, so can accept any number of electromagnetic modes. Readers not familiar with these concepts may wish to refer to a general review of detection technology [1].

Most of the devices discussed in this review depend on The quantum mechanical tunneling between two superconductors. This effect is best understood from studies of tunnel junctions consisting of two thin

superconducting films separated by a several nm thick tunnel barrier made from the oxide of one of the superconductors or other insulating material. Two distinct tunneling phenomena can transport current through such junctions. Josephson, or pair tunneling, results from the overlap of superconducting ground state wave functions in the barrier. Quasiparticle or single particle tunneling arises from the overlap of wavefunctions for the single particle excited states. Superconducting receivers for infrared and millimeter waves depend on the nonlinear response of these currents when driven by constant and RF voltages. This response has been calculated from the theory of superconductivity and has been verified in detail by many experiments. A basic familiarity with these phenomena will be assumed that can be obtained from one of the standard books on superconducting tunneling [2-4]. The time dependent current I(t) resulting from a voltage V across a tunnel junction can be written

$$I(t) = I_c \sin \phi + V[G(V) + G'(V) \cos \phi] + C\, dV/dt. \qquad (1.1)$$

The first term on the right is the lossless Josephson pair tunnel current. It has a maximum value called the Josephson critical current I_c and it depends on the phase difference ϕ of the superconducting order parameter or wave function in the two superconductors. Since the time derivative of this phase is proportional to the voltage,

$$\hbar d\phi/dt = 2\, eV, \qquad (1.2)$$

this first term describes the ac Josephson currents at the frequency $\omega_J/2\pi$ = 2eV/h = 484 GHz/mV. The second term VG(V) of Eq. (1.1) is the quasiparticle current. The third term VG'(V)cosϕ represents an interaction between the pair and quasiparticle currents. The effects of this term on device performance are subtle and it is often neglected for simplicity. Since the junction capacitance C is important at millimeter wave frequencies, the displacement current is included as the final term in Eq. (1.1). The admittance of circuit elements that are coupled to the junction at RF will also be important for device performance.

Many infrared and millimeter wave superconducting devices can be classified as either Josephson effect or quasiparticle devices, depending on whether the important nonlinearity arises from the first or second term in Eq. (1.1). The Josephson effect devices are either operated at zero bias voltage (as with the parametric amplifier) or at finite voltage and very low capacitance (as with the Josephson mixers and detectors). For detailed reasons, the nonlinearity of the quasiparticle conductance G(V) is relatively unimportant in these applications and theoretical models are used in which G(V) in Eq. (1.1) is replaced by the linear conductance R_N^{-1}, and G'cosϕ is neglected. This resistively shunted junction (RSJ) model is used to describe Josephson devices in Section IV below. Quasiparticle devices are generally operated with large enough bias voltage that the Josephson frequency ω_J is well above the signal frequency ω_S, and with sufficient capacitance that $\omega_S R_N C$ is of order unity. The ac Josephson currents are then shunted by the junction capacitance, so do not flow in the external circuit and can largely be neglected. For the high values of ω_S, a magnetic field is often applied to suppress the Josephson current.

The nonlinearity in the quasiparticle conductance G(V) arises from the energy gap of width 2Δ in the density of excited single particle (quasiparticle) states. In an ideal junction at T=0, quasiparticle current can flow only when a bias voltage $V \geq 2\Delta/e$ is applied, so that the filled states on one side of the junction have the same energy as the empty states on the other. Because of the singularities in densities of states at the gap edges, the onset of tunneling current at $2\Delta/e$ has infinite slope in the weak coupling limit of superconductivity theory. When $eV >> 2\Delta$, the quasiparticle conductance approaches the normal state value R_N^{-1}. This onset of quasiparticle current at 2Δ has been called the strongest nonlinearity in nature. In the I-V curve of a real tunnel junction such as is shown in Fig. 1a), there is always some rounding of the corner at 2Δ, and some leakage current is apparent at lower voltages.

The I-V curves of superconductor-insulator-normal metal (SIN) tunnel junctions show no Josephson pair tunneling. The onset of quasiparticle tunneling occurs at Δ/e and is less sharp because there is a singularity in the density of states only on one side of the junction. A type of SIN junction called the super-Schottky diode uses a heavily doped semiconductor as the normal conductor.

II. QUASIPARTICLE MIXERS

Photon Assisted Tunneling

The static I-V curve for a quasiparticle tunnel junction which is pumped by a coherent local oscillator with constant voltage amplitude V_{LO},

$$V = V_o + V_{LO} \cos \omega_{LO} t, \tag{2.1}$$

can be written in the form

$$I(V_o) = \sum_{n=-\infty}^{\infty} J_n^2(\alpha)\ I_{dc}(V_o + n\hbar\omega_{LO}/e). \tag{2.2}$$

This I-V curve has the form of a sum over the dc I-V curves $I_{dc}(V)$ observed without the LO pump, each displaced in voltage by an amount $n\hbar\omega_{LO}/e$, where $n=0,\pm1...$ The amplitude of each term in the sum is $J_n^2(\alpha)$ where $\alpha=eV_{LO}/\hbar\omega$. The sharp onset of quasiparticle tunneling thus causes a series of steps as is shown in Fig. 1(b). These steps are due to photon assisted tunneling. Whenever a multiple $n\hbar\omega$ of the photon energy makes up the difference $(eV-2\Delta)$ there will be an enhancement $(eV<2\Delta)$ or reduction $(eV>2\Delta)$ of the tunneling current. The quasiparticle is said to tunnel with the absorption or emission of one or more photons. Distinct photon assisted tunneling steps are seen only when the onset of quasiparticle tunneling is sharp on the voltage scale $\hbar\omega/e$. At low frequencies or for rounded I-V curves, Eq. (2.2) approaches the classical limit of a dc I-V curve averaged over the LO voltage swing.

When the admittance of the LO source is small, the voltage amplitude V_{LO} of the pump depends on the RF admittance of the junction which, in turn, is a function of the bias voltage for a constant pump power. Negative resistance can occur on photon assisted tunneling steps when the RF admittance of the

pumped junction varies in such a way that V_{LO} decreases with increasing dc bias. The quantum theory of quasiparticle detection and mixing [5] includes the formalism required to calculate pumped I-V curves with arbitrary LO source admittance. The nonlinear quantum susceptance, which is the counterpart of the nonlinear quasiparticle conductance, plays an important role in this theory. The results of such a calculation are shown in Fig. 1(c) for a case in which negative resistance is seen [6].

Quasiparticle Mixing

A heterodyne mixer is generally used to down-convert signals from some high RF frequency to a lower frequency where amplification and further signal processing is convenient. The classical mixer makes use of the nonlinear resistance of a Schottky barrier diode that is strongly pumped by a local oscillator at ω_{LO}. The mixer produces a linear response at the intermediate frequency ω_{IF} when a small signal is supplied at the signal frequency $\omega_S=\omega_{LO}+\omega_{IF}$ or the image frequency $\omega_I=-\omega_{LO}+\omega_{IF}$. In general, currents flow in the mixer at all frequencies $\omega_m=m\omega_{LO}+\omega_{IF}$, $m=0,\pm1\ldots$, where $\omega_S=\omega_1$, $\omega_I=\omega_{-1}$, and $\omega_{IF}=\omega_0$. The mixer performance depends on the admittances Y_m which terminate the pumped junction at all of these frequencies, or ports, as is shown in Fig. 2. In practical SIS mixers the junction capacitance usually provides a high enough admittance that the RF voltage is zero for all ports $|m|>1$. In this case, a three-port theory, which includes only ω_S, ω_I and ω_{IF} is a very useful approximation.

The classical theory of microwave mixers assumes that the instantaneous current I(t) in a nonlinear resistance is determined by the instantaneous

voltage V(t). The single sideband (SSB) conversion efficiency or gain of such a mixer is always less than 0.5. The quantum theory of mixing [5] includes classical mixer theory as a limiting case when the I-V curve is not sharp on the voltage scale $\hbar\omega/e$. When quantum effects are important, this theory predicts many unusual properties for quasiparticle mixers, including large gain and very low noise. The quantum theory is formulated in terms of an admittance matrix $Y_{mm'}$ which relates the current i_m in port m to the voltage $V_{m'}$ in port m'. A prescription is given for calculating $Y_{mm'}$ from V_{LO} and the dc I-V curve of the junction [5]. The coupled mixer gain, $G_{\pm 1}$, is defined as the power coupled to the IF load divided by the power available from an RF source at the signal port (+1) or the image port (-1). It can be expressed in terms of the Z-matrix $[Z_{mm'}] = [Y_{mm'}+Y_m\,\delta_{mm'}]^{-1}$,

$$G_{\pm 1}(\mathrm{SSB}) = 4\mathrm{Re}(Y_{\pm 1})\mathrm{Re}(Y_0)|Z_{0\pm 1}|^2 . \tag{2.3}$$

It is instructive to express the coupled gain $G_{\pm 1}$ in Eq. (2.5) as a product of the available mixer gain $G_{\pm 1}^{o}$ and the IF coupling coefficient C_{IF},

$$G_{\pm 1} = G_{\pm 1}^{o}\, C_{IF}, \tag{2.4}$$

where

$$G_{\pm 1}^{o} = R_D \mathrm{Re}(Y_{\pm 1}) \left|\frac{Z'_{0\pm 1}}{Z'_{00}}\right|^2 . \tag{2.5}$$

Here the dynamic resistance R_D is dV/dI from the pumped I-V curve, and

$$C_{IF} = 1 - \left|\frac{1/Z'_{00} - Y_0^*}{1/Z'_{00} + Y_0}\right|^2 . \tag{2.6}$$

In Eqs. (2.5) and (2.6), Z' is the Z-matrix calculated with an open output $Y_0=0$. Eq. (2.5) suggests that the available mixer gain is approximately proportional to the dynamic resistance R_D of the pumped junction. The available gain can become infinite for infinite or negative R_D. The input admittance of an SIS mixer is of order R_N^{-1}. When the gain is large, the output admittance $(Z'_{00})^{-1} \approx R_D^{-1}$ is $<<R_N^{-1}$. Large coupled gain is observed, therefore [7], only when a transformer is used to provide an IF load impedance significantly larger than 50 Ω.

Many of these predictions regarding mixer gain can be understood from a simple picture. The mixing between the RF signal and the LO can be viewed as a small modulation of the LO amplitude at ω_{IF}. This modulation produces a current I_{IF} in the junction and provides an available IF power of $I_{IF}^2 R_D/4$, resulting in a linear dependence of the mixer gain on R_D. Since R_D is a maximum at the center of each photon assisted tunneling step, the gain is expected to have peaks at these bias points. These features are clear in Fig. 3 which shows the IF output of an SIS mixer as a function of bias voltage.

Mixer Noise

The contribution of shot noise in the tunneling current of the pumped junction to mixer noise was calculated using classical radiation fields [5]. The components of the broad-band shot noise that appear at the frequencies ω_m, $|m| \geq 1$ are downconverted and superimposed on the shot noise in the IF band. Because these contributions to the output noise are correlated, the shot noise in the output of a double sideband (DSB) mixer [9,10] or a mixer with two local oscillators [11] can vanish under certain conditions.

Since frequency down-conversion with unity power gain corresponds to a gain in photon number, heterodyne mixers can be classified as phase preserving linear amplifiers. Arguments related to the Heisenberg uncertainty principle $\Delta n \Delta \Phi > 1/2$ for photon number n and phase Φ show that any such amplifier will add a noise power $\hbar\omega B/2$ for each input port. If each input is terminated by a blackbody with physical temperature T, then the noise power referred to the input contains a term

$$P = \frac{\hbar\omega}{2} \left(1 + \coth \frac{\hbar\omega}{2kT}\right) B \ , \tag{2.7}$$

in addition to the contribution from shot noise [10,12]. The minimum possible noise power for each input port (for T=0 and zero shot noise) is then $\hbar\omega B$. If the mixer noise temperature T_M is defined as the physical temperature of a blackbody that produces the power in Eq. (2.7), then the quantum limit to this noise temperature is obtained by equating $\hbar\omega B = (\hbar\omega B/2) \coth(\hbar\omega/2kT_Q)$, so that

$$T_Q = \hbar\omega/k \ \ln 3 \tag{2.8}$$

Some authors define a noise temperature T_M', which is linear in noise power, by setting Eq. (2.7) equal to $kT_M'B$. For this case $T_Q' = \hbar\omega/k$. Mixers have been built at 36 and 114 GHz that have measured noise temperatures within a factor 2 of T_Q [13,14].

In addition to the intrinsic shot noise and the quantum noise limit, SIS mixers can suffer from noise associated with the Josephson effect. To avoid instabilities caused by the Josephson current at low bias voltages, an SIS mixer has to be biased above a threshold voltage,

$$V_T = V_{LO} + K \left(\frac{\hbar\omega 2\Delta}{e^2 \omega R_N C}\right)^{1/2}, \qquad (2.9)$$

where K is a constant close to unity [5]. Below this threshold the noise is high and the bias point is unstable as is seen in Fig. 3. Because an SIS junction is usually biased at ~$\hbar\omega/2e$ below the gap, this threshold is a problem for SIS mixers at high frequencies. To avoid this instability a magnetic field is often used to quench the Josephson currents. Other possibilities include using SIS junctions with magnetic impurities in the tunnel barrier to suppress the pair tunneling, and using SIN junctions which do not have pair tunneling.

Imbedding Admittance and Computer Modeling

For optimum SSB gain, the imbedding susceptance at ω_S should resonate the susceptance of the pumped junction, which arises from both the nonlinear quantum susceptance and the geometrical junction capacitance. Also, the imbedding conductance at ω_S should match the RF conductance. For DSB mixers, these conditions must be met at both ω_S and ω_I. Waveguide mixers generally have $\omega_S R_N C \geq 2$ so only three mixer ports are important, and one or more mechanical tuning elements are used to obtain good RF coupling. Planar lithographed quasi-optical mixers are sometimes operated with $\omega_S R_N C \sim 1$ to provide good coupling to a resistive RF source. In this case harmonic response can be important. Alternatively they operate with $\omega_S R_N C \geq 2$ and are provided with lithographed RF matching structures.

The quantum theory of mixing [5] can be used to compute the performance of an SIS mixer if the I-V curve, the dc and LO bias and the imbedding admittances are known. The unpumped I-V curve, dc bias, and available LO power can be measured directly. The theory includes a prescription for calculating V_{LO} from the available LO power. As with classical mixers, however, it is difficult to obtain adequate information about the IF and RF imbedding admittances.

Waveguide mixers for millimeter waves are often designed using lower frequency (3-12 GHz) measurements on large scale models. Scaled modeling has not yet been used for planar lithographed mixers which use RF matching structures that rely on the properties of superconductors. The geometries used in these structures, however, are often selected to facilitate direct calculations of the RF imbedding admittances.

The dependence of the shape of the pumped I-V curve on the LO source admittance shown in Fig. 1(b) and (c) can be used to deduce values for the RF admittance. The original technique [15] used the available pump power and the dc current to obtain allowed values of Y_{LO} in the form of circles in the admittance plane. If the input data are very precise, Y_{LO} can be obtained from the intersection of several circles. More recently, considerable success has been obtained with an automated computer search for the value of Y_{LO} which produces the best fit to an experimental pumped I-V curve, as is shown in Fig. 1c) [6].

A number of attempts have been made to compare calculations of mixer performance from quantum mixer theory with direct measurements of gain and noise. All of the qualitative effects predicted by theory have been observed. Predictions of gain have been quite successful [5] when the onset of quasiparticle tunneling is not very sharp on the voltage scale $\hbar\omega/e$. Predictions of noise are less successful, but still frequently agree within a factor 2. Substantial disagreements between theory and experiment are often found when the I-V curve is very sharp, especially with regard to the conditions under which infinite gain is available [13]. It is possible that comparisons in the quantum limit are particularly sensitive to errors in the imbedding admittances.

LO Power and Saturation

An estimate of the V_{LO} required to pump a mixer biased on the nth photon step can be obtained from the value of $\alpha_n = eV_{LO}/\hbar\omega$ which corresponds to the first maximum of $J_n(\alpha)$. Since the input impedance of an SIS mixer is of the order of its normal resistance R_N,

$$P_{LO} \approx (N\hbar\omega\alpha_n/e)^2/2R_N \ . \qquad (2.10)$$

This equation includes the case of a mixer which uses a series array of N junction with total normal resistance R_N. The relation (2.10) is found to account for the observed P_{LO} to within 2dB for experimental values which range from 1nW for single junction mixers to 30μW for array mixers [5]. These low values of P_{LO} are a great convenience for SIS mixers, especially at

submillimeter wave frequencies. It appears possible that the Josephson local oscillator described in Section IV can be used to pump an SIS mixer.

Because of the small values of P_{LO} required, quasiparticle mixers saturate at relatively low signal levels. For this reason, SIS mixers are limited to small signal applications. Saturation first occurs in the mixer output because of the rapid dependence of mixer gain on bias voltage shown in Fig. 3. The IF response of the mixer can be viewed as a modulation of the instantaneous bias point at frequency ω_{IF}. When the amplitude V_{IF} of this IF voltage swing reaches some fraction γ of the width $N\hbar\omega/e$ of the gain peak, the average gain is suppressed. If the mixer is matched at the IF output, the input RF power that will cause saturation can be written

$$P_{sat} = (\gamma N\hbar\omega/e)^2/2GR_D \ . \qquad (2.11)$$

For a single junction mixer with $R_D=50\Omega$, G=3dB and $\gamma=0.1$ (which corresponds to 0.2dB gain compression) this expression gives $P_{sat}=2pW$, in agreement with a measured value of 1.5pW [5]. For a quantum noise limited mixer with unity gain and a 500 MHz IF bandwidth, the dynamic range is 20dB at 36 GHz. This is large enough for most astronomical applications. However, it might be insufficient for radar and communication systems.

Although problems with saturation from 300K noise can occur in broad-band SIS mixers, such extreme problems can be avoided by several techniques. The use of a series array of N junctions will increase P_{sat} by N^2. Also, if the coupled RF bandwidth is larger than ω_{IF}, then the V_{IF} that comes from a

broad-band signal can be reduced by the use of a low pass filter that shorts the mixer output for frequencies above ω_{IF} [16].

Series Arrays of Junctions

Some freedom is introduced into the design of quasiparticle mixers by the possibility of using arrays of junctions in series. If the RF currents have the same phase in N identical junctions, then the equivalent circuit of the N-junction array can be reduced to that of a single effective junction with normal state resistance and series inductance increased by the factor N and capacitance decreased by the same factor. The voltage scale of the I-V curve is increased by the factor N. If junctions with the same tunnel barrier are used, the response time R_NC is unaffected. In order to retain impedance matching at RF and IF, the junctions in the array should have areas N times larger than for the single junction mixer. Measurements of the performance of array mixers scaled in this way show that mixer gain and noise can be independent of N up to at least N=25 [17].

Advantages of array mixers include a saturation level and dynamic range which scale as N^2, and junction areas which scale as N. The relaxation of fabrication requirements for the larger junctions is partly offset, however, by the need for nearly identical junctions. One disadvantage of array mixers is that the series inductance L of the array scales as N. Limits to the operating frequency ω_S of SIS mixers set by $(LC)^{-1/2}$ or R_N/L can be troublesome when arrays are used at high frequencies.

Types of Junctions

The SIS quasiparticle mixer depends on the availability of tunnel junctions with a well defined onset of quasiparticle current at $V=2\Delta/e$, values of resistance $20 \leq R_N \leq 100\ \Omega$ that can be matched at RF and IF frequencies, and small enough capacitance that the relaxation time R_NC can meet the criterion $1 \leq \omega_S R_N C \leq 10$. When $\omega R_N C$ is held fixed, the Josephson critical current density, which is an exponential function of barrier thickness, scales directly with frequency; it is ~500A/cm^2 at 100 GHz. Since the spread of useful barrier thicknesses is only 10%, the specific capacitance depends only on the type of barrier used. The value of 40 fF/μm^2 for the oxides of Pb-In alloys [18] and 45 fF/μm^2 for Al_2O_3 [19] and the value of 140 fF/μm^2 for the higher dielectric constant oxides of Nb [18] and Ta [13] can be used for design purposes. The junction areas required scale inversely with operating frequency and are typically 1-4 μm^2 at 100 GHz.

A variety of approaches have been used to fabricate the small junction areas required. These include photoresist lift-off to produce window junctions with areas of 1-4 μm^2, photoresist bridge masks to produce overlap junctions with areas of 0.5-2μm^2, and edge techniques for areas less than 0.5μm^2.

Most early mixer experiments made use of Pb-alloy junctions with In-oxide barriers. These junctions usually degrade gradually when stored at room temperature. Junctions made from Nb/Nb-oxide/Pb-alloy are more durable, but suffer from the higher dielectric constant of the Nb-oxide. All-Nb junctions with artificial barriers such as Al_2O_3, MgO and α-Si are becoming available that combine ruggedness with a low barrier dielectric constant. A few experiments have been done with Sn/Sn-oxide/Sn and Ta/Ta-oxide/Pb-alloy

junctions which have very low leakage current and a very sharp onset of quasiparticle tunneling.

The requirement of small current flow at voltages below $2\Delta/e$ sets an upper limit of $\sim T_c/2$ on the operating temperatures that can be used for SIS mixers. Since there are significant conveniences to operation with unpumped LHe at 4.2K, or with mechanical refrigerators (which achieve temperatures below ~4.5K only with difficulty) there are benefits from the use of Nb junctions with T_c=9K compared with ~7K for the Pb alloys. In the future, the cryogenic problem will be eased by the availability of NbN junctions with T_c=15K.

It is interesting to speculate on the usefulness of SIS quasiparticle mixers made from the new superconductors with much higher values of T_c. In the radio astronomy applications, higher operating temperatures would be an advantage only if the noise temperature does not also increase. The noise temperatures of receivers that use cooled Schottky diode mixers are less than 10 times those of the best SIS receivers at W-band. The energy gap limitation to the operating frequency of SIS mixers could be significantly relaxed by the use of high T_c superconductors. Operation at frequencies above one THz, however, will require extremely small junctions with area $<0.1\mu m^2$ and very high current densities $>10^5 A/cm^2$. At present there is no appropriate high T_c SIS junction technology.

Quasiparticle Mixer Measurements

Measurements of the performance of SIS receivers are generally made by coupling in signals from hot and cold loads at ~300K and 77K, and by measuring the output of the cold IF amplifier on a spectrum analyzer. Coherent sources are used to test the relative gains for the signal and image ports. A

bi-directional coupler is frequently introduced at the output of the mixer to measure the impedance mismatch at the output, which is important for receiver optimization. A coherent IF signal from an external source can then be reflected from the mixer output to evaluate the IF coupling and signals can be introduced to measure the gain and bandwidth of the IF amplifier. The complications of cryogenic operation make it difficult to obtain the accurate measurements of the performance of the isolated mixer that are required to test quantum mixer theory. Special techniques such as cryogenic hot-cold loads at both the RF and IF ports have been developed for this purpose [20].

Performance of Waveguide SIS Mixers and Receivers

Soon after the first mixing experiments were reported in 1979, SIS quasiparticle mixers began to replace Schottky diode mixers in coherent receivers for molecular line radio astronomy [21-23]. These receivers are now in daily use on millimeter wave telescopes and interferometers in at least six observatories. Portable line receivers for submillimeter wavelengths are being developed for use on mountain top and airborne telescopes. Other applications include atmospheric line measurements and radiometers for measurements of the anisotropy of the cosmic microwave background [24]. The SIS quasiparticle heterodyne mixer is now the technology of choice for sensitive coherent receivers from the upper limit of high electron mobility transistor (HEMT) amplifiers [25] at ~40 GHz to more than 800 GHz.

More than one hundred papers have been published describing the performance of SIS quasiparticle mixers and receivers. A few highlights of these developments will be described here, starting with the waveguide mixers which are typically used at frequencies below ~400 GHz.

Good coupling to both the real and imaginary parts of the RF mixer admittance is most easily obtained by the use of a waveguide mount with two mechanical adjustments. Early evaluations of the potential of SIS mixers done in this way gave significantly better performance than was obtained from early mixer blocks with one mechanical adjustment.

Much attention has been given to careful optimization of W-band mixers (75-110 GHz) to achieve broad instantaneous bandwidth, broad tuning range and optimum termination of the image and harmonic ports. Current practice often makes use of integrated tuning elements lithographed on the junction substrate, which can take the form of lumped or distributed circuit elements [26-28]. An example of such a mixer with two mechanical tuning elements [14] is shown in Fig. 4. A broad tuning range with good instantaneous bandwidth has also been obtained with only one mechanical adjustment by the use of suitable lithographed tuning elements [27].

The lowest noise and highest gain thus far obtained from SIS mixers have come from waveguide devides. One experiment in K_A band at 36 GHz with very high quality Ta junctions and two experiments at 100 GHz with Pb-alloy junctions gave noise temperatures of T_m(SSB)=3.6K [13], T_m(DSB)=6.6 [14], and 5.6K [27], respectively, which are within a factor two of the quantum limits for these frequencies. Measurements of a W-band mixer with a small IF load admittance gave values of coupled gain as large as 12.5dB [7]. The observation of such large coupled gain is an interesting confirmation of quantum mixer theory. Because of the low noise available from HEMT IF amplifiers, however, gains of order unity are more appropriate for practical receivers.

Despite the progress that has been made in optimizing W-band SIS quasiparticle receivers, the noise temperatures of the receivers on telescopes are a factor 10 or more above the quantum limit. There is room for improvement before the sky temperature limit is reached. A summary [22] of some of the best reported results is shown in Fig. 5.

Waveguide SIS mixers have been constructed at frequencies up to 345 GHz by several groups [13,14,23,27,29,30]. Because of increased waveguide loss and increased difficulty of fabricating precise structures for these frequencies, simpler mixer blocks are often used with a single mechanical adjustment and a circular waveguide as is shown in Fig. 6. Many of the best results have been obtained by operating at $\omega R_N C \lesssim 1$ with submicron junctions and no lithographed tuning elements. Although the noise temperatures of these receivers shown in Fig. 5 do not approach the quantum limit as closely as do the W-band receivers, their performance is good enough to produce very valuable astronomical data.

Interference from Josephson tunneling phenomena becomes increasingly troublesome as the operating frequency is increased. Even in a magnetic field, the value of P_{LO} must sometimes be limited so that the instability described in Eq.(2.9) does not interfere with operation on the first photon step below the gap. An encouraging noise temperature of $T_M(DSB) \approx 200K$ has been obtained at 230 GHz with an SIN mixer [31] which avoids this problem.

Quasioptical SIS Receivers

Thin film SIS tunnel junctions are compatible with other lithographed superconducting receiver components such as planar antennas, transmission

lines, and filters. It is therefore attractive to use optical lithography to make integrated planar quasioptical receivers at high frequencies so as to avoid the fabrication problems associated with waveguide structures. Since planar antennas located on a dielectric surface radiate primarily into the dielectric, the RF signals are introduced through the back surface of the dielectric, which curved to form a lens as is shown in Fig. 7. Early work on planar integrated SIS mixers began with bow-tie antennas, but attention has shifted to log-periodic and spiral antennas which have more symmetrical central lobes and so can couple more efficiently to telescopes. All three are self-complementary and so have real impedances of 120 Ω when deposited on quartz.

As is shown in Fig. 5, very good performance has been obtained over the extremely broad bandwidth from 100 to 760 GHz with a planar quasioptical SIS receiver [22]. This mixer used a single Pb-alloy junction with $\omega_S R_N C=1$ at 300 GHz and a spiral antenna. Saturation on 300K noise was avoided by shorting the mixer output for frequencies above ω_{IF}.

The future appears very bright for planar quasioptical SIS mixers for frequencies up to and beyond 1 THz, especially if junctions can be made from high T_c superconductors such as NbN (which can have $\omega_S R_N C\sim 1$ at 1 THz) with small enough areas to match the antenna resistance. These severe requirements on junction fabrication can be eased by the use of lithographed matching structures such as those shown in Fig. 8. These structures have been used on planar quasioptical mixers with bow-tie and log-periodic antennas at frequencies from 90 to 270 GHz [32,33]. They are used to resonate the junction capacitance over RF bandwidths of 5-25 percent and thus to permit the efficient

use of junctions with $\omega_S R_N C \lesssim 10$. Since conventional microwave test apparatus is not available at such high frequencies, special techniques are used to evaluate the RF coupling provided by such structures. These have included using a Fourier transform far-infrared spectrometer as a sweeper and the mixer junction a direct detector [34].

III. QUASIPARTICLE DIRECT DETECTOR

Theory

The quasiparticle direct detector, also called a video or square-law detector, uses the nonlinearity of the quasiparticle I-V curve of an SIS junction to rectify the coupled RF signal. The current responsivity of such a detector is defined as the induced dc divided by the available signal power $S_I = \Delta I_{dc}/P_S$. In the quantum theory [5] the current responsivity is obtained from the small signal limit of the theory of the pumped I-V curve in Section II,

$$S_I = \frac{e}{\hbar\omega} \left[\frac{I_{dc}(V_o+\hbar\omega/e) - 2I_{dc}(V_o)+I_{dc}(V_o-\hbar\omega/e)}{I_{dc}(V_o+\hbar\omega/e) - I_{dc}(V_o-\hbar\omega/e)} \right] . \tag{3.1}$$

If the RF source is not matched to the detector, an RF mismatch factor must be included. The quantity in the square brackets in Eq.(3.1) is the second difference of the unpumped I-V curve computed for the three points $V=V_o$ and $V_o \pm \hbar\omega/e$, divided by the first difference computed at $V=V_o \pm \hbar\omega/e$. In the classical limit, where the current changes slowly on the voltage scale $\hbar\omega/e$,

the differential approximation gives the usual result for a diode detector $S_I=(d^2I/dV^2)/2\ (dI/dV)$. If the I-V curve is sharp enough that the current rise at 2Δ occurs within the voltage scale $\hbar\omega/e$ and if the bias voltage V_o is just below $2\Delta/e$, then Eq.(3.1) becomes $S_I=e/\hbar\omega$. This quantum limit to the responsivity corresponds to one extra tunneling electron for each coupled photon. The SIS direct detector makes a continuous transition between the classical energy detector and the quantum photon detector.

Since direct detectors do not preserve phase, there is no quantum limit to the detector noise analogous to that for the mixer. The intrinsic noise limit of the quasiparticle direct detector is the shot noise $\langle I_N^2\rangle=2eI_{dc}(V_o)B$ in the dark current I at the bias point. Here B is the post-detection bandwidth. The noise equivalent power (NEP) in $WHz^{-1/2}$ of an RF-matched SIS direct detector is then

$$NEP = \langle I_N^2\rangle^{1/2}/S_I B^{1/2} = [2eI_{dc}(V_o)]^{1/2}/S_I \ . \qquad (3.2)$$

In the quantum limit, the NEP increases linearly with signal frequency ω_S.

When the signal power is increased, the responsivity of an SIS detector falls [35] as $1-P_S/P_{sat}$, where

$$P_{sat} \approx 16[(\hbar\omega/e)^2/2\ R_{RF}] \ . \qquad (3.3)$$

This expression for saturation power is $16G/\gamma^2N^2$ times the corresponding Eq.(2.11) for an SIS mixer. For a single junction mixer this factor is $\sim 10^3$. It can be significantly smaller for mixers made with many junctions in series.

Series arrays of junctions are not useful for SIS detectors, because the responsivity is reduced and the NEP increased by the factor N.

Detector Performance

The first experimental test of an SIS direct detector [36] showed excellent agreement with the quantum theory. The current responsivity of 3.6×10^{3}A/W was within a factor 2 of the quantum-limited value $e/\hbar\omega$ at 36 GHz. Similar results are reported at W-band. In these experiments, the shot noise was measured with amplifiers at 50 MHz and 1.4 GHz which were designed for use as IF amplifiers for heterodyne mixers and found to agree with theory. The NEP was deduced to be 2.6×10^{-16}WHz$^{-1/2}$ at 36 GHz [36], which is essentially equal to the performance of a millimeter wave astronomical radiometer based on the ^{3}He-cooled composite bolometer. In the usual radiometric applications the signal is modulated at some low frequency $1<f<100$ Hz. A receiver for such signals is sensitive to 1/f noise at the frequency f, which is commonly observed in tunnel junctions. Also, an amplifier at frequency f must be used that does not contribute significant excess noise for a source resistance of a few hundred ohms. Even if these problems are solved, an astronomical radiometer based on the SIS direct detector will not be significantly more sensitive at millimeter wavelengths than the SIS heterodyne radiometer which uses a Schottky diode detector at the output of the IF amplifier. It will be less sensitive at submillimeter wavelengths than the ^{3}He-cooled bolometric radiometer.

The potential remains for applications of the SIS direct detector at near-millimeter and submillimeter wavelengths which benefit from its higher operating temperature and faster speed when compared with the composite

bolometer. It is easier to make in planar arrays than either the composite bolometer or the SIS mixer.

A novel radiometer configuration has been suggested [37] which uses one SIS junction pumped with an LO as a heterodyne downconverter followed by a second SIS junction used as a photon detector. From one viewpoint, the mixer is a preamplifier for the photon detector. It amplifies the photon rate by the product of its power gain and the frequency downconversion ratio. The SIS photon detector is used at the relatively low IF frequency where its NEP is better than at the RF. From another viewpoint, this system is a simplified version of a heterodyne radiometer that avoids the need for the IF amplifier because of the conversion gain of the SIS mixer and the excellent performance of the SIS direct detector. This configuration appears to have higher sensitivity than the SIS direct detector while retaining its high speed and operating temperature. It appears to be simple enough that planar integrated arrays of detectors are possible.

IV. JOSEPHSON EFFECT RECEIVER COMPONENTS

Josephson Effect Detectors and Mixers

Detectors and mixers based on the Josephson pair tunneling currents were explored before the invention of the corresponding quasiparticle devices. Relatively little progress has been made on Josephson effect detectors and mixers in recent years. As a result, detailed early reviews of this subject are still useful [38].

The Josephson effect detector and mixer use junctions with small enough capacitance that $\omega_g R_N C<1$, at the gap frequency $\omega_g=2\Delta/\hbar$. In this limit, the

instantaneous bias voltage oscillates at ω_J, and the time average of the pair current from Eqs.(1.1) and (1.2) does not average to zero for V>0. Because of this Josephson contribution to the dc, such junctions have no hysteresis. This is in contrast to the junctions used for quasiparticle devices which have large enough capacitance that the voltage at the Josephson frequency remains fixed. As a result, the pair currents are sinusoidal and average to zero for V>0, giving hysteretic I-V curves. In practice, point contact junctions or thin film bridges are used to obtain the low capacitance required for the Josephson devices. Figure 9 shows the static I-V curves for a Nb point contact junction (a) without and (b) with an RF pump at 36 GHz [39]. The excess dc above the current V/R_N arises from the time average of the pair current. The Josephson steps in (b) have voltage separation $\Delta V=\hbar\omega_{LO}/2e$, which is half the separation of the photon-assisted tunneling steps in the quasiparticle current. They arise from mixing of the ac Josephson currents at $\omega_J=2eV/\hbar$ with harmonics of the RF pump. Both curves are well described by the RSJ model in which the quasiparticle conductance is assumed to be R_N^{-1}.

The detector and mixer are biased with load lines as shown in Fig. 9(a) and (b). When a small RF current $I_{RF}<<I_C$ flows through the junction, the zero voltage current decreases as I_{RF}^2 [38]. When the Josephson critical current I_C decreases, the I-V curve in the neighborhood of the bias point is shifted downward. This causes an increase in the static junction voltage that is proportional to the negative of the change in I_C and also to R_D at the bias point. The result is a square law or direct detector. Theoretical estimates of the NEP for this device give results which are similar at millimeter wavelengths to the measured performance of the SIS direct detector. The best measured performance was NEP$\simeq$3 and 5×10^{-15} $W\cdot Hz^{-1/2}$ at 90 and 120 GHz. The

NEP increases as $(\omega_S/\omega_C)^2$ at higher frequencies, where $\omega_C=2eI_CR_N/\hbar$ is a cutoff frequency. Since $I_CR_N \approx 2\Delta$, $\omega_C/2\pi \approx 1.5$ THz for Nb junctions. This rapid degradation of the NEP should be compared with the more favorable linear dependence on ω_S for quasiparticle direct detectors with the quantum limited responsivity.

When sufficient RF power is applied that $I_{RF} \simeq I_C/2$, the static junction current decreases linearly with I_{RF}. When both a large LO current and a small signal current are applied, the amplitude of the total current $I_{RF}=I_{LO}+I_S$ oscillates at ω_{IF} with amplitude given by I_S. If the load line at the IF frequency is as shown in Fig. 9(b), the result is a linear heterodyne mixer. The gain in this mixer peaks at bias points where the dynamic resistance is large, as is shown in Fig. 9(c). The gain can exceed unity under favorable circumstances.

The general principles of operation of the Josephson-effect mixer have been well reviewed [38] so will not be discussed in detail here. Mixer performance, including noise, has been carefully analyzed using analog simulations and digital calculations. When a realistic model of the microwave imbedding network is included, the mixer noise T_M is significantly larger than either the quantum noise $\hbar\omega/k$, or the ambient temperature. The cause of this noise is the efficient harmonic mixing displayed by the Josephson-effect mixers. Broad-band noise in the mixer at RF frequencies, whether thermal or photon in origin, is mixed down into the IF band by beating with many harmonics of the LO frequency and with the ac Josephson frequency [40].

Optimization of Josephson-effect mixers is difficult because the performance depends on the imbedding admittances at many combinations of ω_J,

ω_S, ω_I and ω_{LO}. Careful evaluations of Josephson mixers have been carried out from 36 to 450 GHz. Over this range the best values of SSB gain decrease from 1.4 to 0.3, and the T_M(SSB) increases from 54 to ~1000 K [39,41,42,43]. The conversion gain is expected to decrease as $(\omega_c/\ \omega_S)^2$ at high frequencies. Harmonic mixing in Josephson mixers is relatively efficient, even for high harmonics [38].

As with the direct detector, the performance of the Josephson mixer is somewhat worse than its quasiparticle counterpart. A major problem with these Josephson devices is that to operate at any signal frequency they require smaller values of junction capacitance than the quasiparticle devices require for operation at THz frequencies. Thin film tunnel junctions with such low capacitance have been made with difficulty, but are fragile, and have not been used successfully for mixing. Thin film bridges [2,3] can be used in principle, but have not been a real success, partly because the bridges used did not have the full theoretical value of the I_cR_N product. Accidental junctions such as those encountered in granular films have also not been successful.

There is current interest in Josephson mixers using accidental junctions in high T_c superconductors. Mixing is easy to observe, but competitive performance has not been demonstrated. Since the ratio of T_M to the operating temperature is at least 10 in the best Josephson mixers, millimeter wave high T_c mixers operated above LHe temperatures will probably be noisier than cooled Schottky mixers, which can have T_M as low as 120 K at 90 GHz. High frequency Josephson mixers are possible in principle because of the high cutoff frequency, but junctions problems will remain severe.

Josephson Local Oscillator

Considerable attention has been given to the possibility that the oscillations of the Josephson current at 484 GHz/mV can be used for a practical voltage-controlled oscillator (VCO) for millimeter and submillimeter wavelengths. Possible applications include tunable integrated local oscillators or pumps for quasiparticle mixers or Josephson parametric amplifiers. The existence of such an oscillator might make it possible to produce an entire receiver on a single chip, including a planar antenna, local oscillator, mixer and amplifier.

Calculations [44] based on the RSJ model show that the maximum power radiated by a junction into a matched transmission line is

$$P_{max}=0.4\ I_C V \approx 0.4V2\Delta/eR_N\ , \tag{4.1}$$

for frequencies below the cutoff frequency, $\omega_c/2\pi$. This power increases with decreasing R_N.

Thermal fluctuations in the quasiparticle resistance modulate the linewidth of the Josephson oscillator. In the RSJ approximation the FWHM linewidth can be written [44]

$$\Delta\omega = 8\pi^2 R_D^2 kT/R_N\Phi_o^2\ , \tag{4.2}$$

where Φ_0 is the flux quantum h/2e. Since the dynamic resistance at the bias point R_D scales with R_N, this linewidth increases linearly with R_N.

In order to use an oscillator with limited power to pump a mixer or parametric amplifier, it is necessary to use a diplexer which will couple both the oscillator and the signal source with high efficiency over the required

bandwidth. This condition is more easily met if the oscillator output impedance is comparable to the RF source impedance, which is ~100Ω for a planar antenna. For a R_N=100Ω Nb junction, P_{max}=3nW at 100 GHz. This power is slightly less than that required to pump an SIS mixer. The bandwidth predicted from Eq.(4.2) is ~16 GHz for a 100Ω junction at 4.2K. This linewidth is too wide for most applications. The experimental linewidths are several times broader because of the effects of other noise sources.

An oscillator based on a single 2×2 μm^2 NbN/MgO/NbN junction with R_N=2Ω has been used to pump a 110Ω tunnel junction [45]. Despite the impedance mismatch, the coupled LO power of 10nW at 500 GHz was sufficient to create well developed photon assisted tunneling steps. The linewidth is estimated from Eq.(4.2) to be 160 MHz, which is narrow enough for some SIS receiver applications. This technology could be used to make an integrated superconducting oscillator and mixer if a way is found to prevent the oscillator from short-circuiting the mixer at ω_S.

Series arrays of Josephson junctions produce more power and narrower linewidths than single junctions. If all of the junctions oscillate at the same frequency and with the same phase, P_{max} is N^2 times that in a single junction with the same resistance as the array and the linewidth is N-times narrower [44]. Phase locking can occur despite variations in the critical current or resistances of individual junctions, if the bias voltage is exactly the same on all junctions.

In the oscillator circuit [46] shown in Fig. 10, the oscillator junctions are connected in series, one wavelength apart, along a superconducting microstrip line. This line drives a resistive load in series with a detector junction. Both ends of the line are terminated in open-ended λ/4 stubs. The

input and output for the dc bias are connected alternately to the line midway between the junctions where there are nodes in the RF current. Because each neighboring pair of junctions is connected in a superconducting loop, the bias voltage on one junction is equal and opposite to the voltage on its neighbor. With all 40 junctions of the array phase-locked, ~1μW of power was delivered to a 60Ω load in a ~10% tunable bandwidth from 350-380 GHz [46].

A second approach to the oscillator problem is called the flux flow oscillator [47]. A static magnetic field is applied in the plane of a Josephson junction which is long compared to its width in the direction of the field. This field creates a linear array of flux vortices in the junction which move due to the inverse Lorentz force when the junction is biased. In an experimental oscillator [47], the moving vortex lines drive RF through a detector junction which is dc isolated so that it can be separately biased. The frequency of this oscillator is given by the Josephson relation $\omega_J=2eV/\hbar$ and the power is a sensitive function of the magnetic field. Using a ~1mΩ oscillator junction, 1μW was coupled to a 2Ω detector junction over a very broad tuning bandwidth from 100-400 GHz. Because of the low resistance of the oscillator junction, the linewidth estimated from Eq.(4.2) is 160 KHz.

It appears that Josephson oscillators can have most of the properties required for use in an integrated receiver. The linewidth, however, remains a problem for many applications. The linewidth increases linearly with operating temperature, so would be worse in an oscillator that uses high T_c superconductors above LHe temperatures. In principle, the high cutoff frequency of high T_c materials could be used to extend the frequency range of Josephson oscillators, if the required structures can be fabricated and the ac losses are sufficiently small.

Josephson Parametric Amplifier

If the current-phase relationship $I=I_c \sin\phi$ for pair tunneling from Eq.(1.1) is combined with Eq.(1.2) the Josephson response of a tunnel junction can be written in the form of a nonlinear inductance $L_J=\hbar/2eI_c\cos\phi$. Parametric devices based on such nonlinear reactances conserve photon number, so the power conversion efficiency is proportional to the ratio of final to initial frequency. Consequently, nonlinear reactors are used for up-conversion and amplification. Downconverters such as the quasiparticle or Josephson mixer, however, use nonlinear resistances which provide a gain in photon number.

Josephson parametric amplifiers can be operated with an external pump, or by using the ac Josephson currents as an internal pump. Because of the narrower pump linewidth, the externally pumped amplifiers achieve better performance [48,49]. When a junction is pumped at ω_p and biased with I=V=0, the result is a four-photon parametric amplifier with $\omega_S+\omega_I=2\ \omega_p$. When the junction is biased with $0<I<I_c$, the result is a three photon amplifier with $\omega_S+\omega_I=\omega_p$.

A Josephson junction is a two terminal device so the input port is the same as the output port. The voltage reflection coefficient is

$$\Gamma = \frac{Z_J - Z_S}{Z_J + Z_S}, \tag{4.3}$$

where Z_J is the impedance of the pumped junction and Z_S is the source impedance at ω_S. To separate the input from the output, a circulator is used as is

shown in the equivalent circuit in Fig. 11. To achieve a power gain $|\Gamma|^2>1$, with a resistive source Z_S, Z_J must be a negative resistance and its magnitude

$$|Z_J| \approx \hbar\omega_p/2eI_c \ , \tag{4.4}$$

must be of order Z_S. To minimize the effects of thermal noise, the Josephson coupling energy $\hbar I_c/2e$ [2-4] must be much larger than the thermal energy kT. For the ratio $\hbar I_c/2ekT=100$ at T=4.2K this critical current is I_c~20 μA, which gives $|Z_J|$~1Ω for ω_p=10 GHz. In order to obtain significant gain from Eq.(4.3) a transformer must be used to reduce $|Z_S|$ to ~1Ω. As is the case with the SIS mixer, the junction capacitance C must be resonated by an inductance L at the signal frequency $\omega_S=(LC)^{-1/2}$ so that Z_J is mainly determined by the nonlinear Josephson inductance. This parallel inductance was also found to be important for stable operation with Josephson parametric amplifiers. Early Josephson parametric amplifiers were troubled by broad-band noise that resembles the chaotic behavior of other nonlinear dynamical systems. It has been shown [4,48] that the parameter range for stable operation is

$$2eI_cL\omega ZC/\hbar \lesssim 1.5\text{-}2.0 \ , \tag{4.5}$$

where Z is the impedance seen by the nonlinear Josephson inductance at resonance.

Noise temperatures as low as 4.5±3 K (DSB) with 13 dB of gain have been obtained at 9 GHz in a 3-photon parametric amplifier operated in pumped L^4He [49]. A similar amplifier operated at 19.4 GHz and cooled to 100 mK gave a

noise temperature of only 0.28 K. This amplifier was used to produce a squeezed state in the noise from a 4.2 K load [50].

The low noise of the Josephson parametric amplifier makes it a candidate for an RF amplifier at the front end of a millimeter-wave receiver or as an IF amplifier at the output of a mixer. Like other superconducting devices, however, the saturation threshold of this amplifier is rather low compared to semiconductor amplifiers. Series arrays of junctions can be used to increase the dynamic range.

Good performance is expected from the Josephson parametric amplifier up to at least 100 GHz in Nb junction technology. As with other Josephson devices, the frequency range over which good performance is expected scales with $\omega_C = 2eI_C R_N/\hbar$. Because these amplifiers are quiet at LHe temperatures, there are prospects for useful performance at higher temperatures and/or frequencies if the required junctions can be fabricated from high Tc superconductors.

V. MULTIMODE DIRECT DETECTORS

Superconducting Bolometer

A bolometric detector consists of a radiation absorber attached to an electrical thermometer with a combined heat capacity C, both connected to a heat sink at temperature T_o via a thermal conductance G. Bolometric detectors with a wide range of sensitivities are used from visible wavelengths to microwaves for sensitive direct detection and for absolute power measurements. Bolometers are also used to detect phonons and X-rays and for detection of high energy particles. The best known superconducting bolometer uses the temperature dependence of the resistance of a superconducting films near T_c as the thermometer.

The infrared power P_{IR} falling on a cold bolometer from a background source with temperature T_B can be obtained from Planck's law if the throughput $A\Omega$ and the spectral bandpass of any cold infrared filters are known. In order to operate the bolometer at the temperature T_c, the thermal conductance must be $G=P_{IR}/(T_c-T_o)$. The saturation power of the bolometer will be $P_{sat}=G\delta T=P_{IR}\ \delta T/(T_c-T_o)$, where δT is the width of the linear part of the resistive transition. If thermal feedback is neglected for simplicity, the voltage responsivity of a bolometer is $S_V=IR\beta/G(1+i\omega\tau)$, where I is the bias current, R is the resistance at the midpoint of the transition, $\beta=d\ell nR(T)/dT$, $\tau=C/G$ is the thermal time constant, and ω is the modulation frequency of the signal to be detected. Since a current-biased bolometer, with $\beta>0$ becomes unstable for large bias, there is a stability condition $I^2R\beta/G=a<1$; a typical value for a is 0.3. The magnitude of β is smaller for semiconductor

thermometers than for superconducting thermometers, but since $\beta<0$ much larger bias currents can be used. Since $\beta\approx\delta T^{-1}$, the square of the responsivity can be written $|S|^2=aR/G\delta T(1+\omega^2\tau^2)$. The NEP of the bolometer can be computed by summing the squares of the statistically independent contributions,

$$NEP = \left[\frac{4k_B^5 T_B^5 A\Omega}{c^3 h^3} \int_0^\infty \frac{t^4 e^t dt}{(e^t-1)^2} + 4k_B T_c^2 G + \frac{4k_B T_c R}{|S|^2} \right.$$

$$\left. + \frac{AV^2}{f|S|^2} + \frac{4k_B T_N R}{|S|^2} \right]^{1/2} . \qquad (5.1)$$

The first term in the square bracket represents the photon noise in the incident radiation for a bolometer with perfect optical efficiency. The second is phonon noise due to the exchange of phonons between the bolometer and the heat sink. Taken together, these terms provide a fundamental limit to the sensitivity of any broad band bolometer with the given values of T_c and T_o. The third term is the limit imposed by the Johnson noise in the thermometer, which has a voltage spectral density $4k_BT_cR$. The fourth term arises from the 1/f noise in the film, which is assumed to have a spectral density of the form $S_V(f)=AV^2/f$, where A is a measured quantity that depends on the properties of the film. The last term is the noise associated with an amplifier with noise temperature T_N used to read out the thermometer.

Amplifier systems are available that make the last term less than Johnson noise, except when T_0<1K and R~1Ω. The 1/f noise is not usually a problem in films of high quality. When heating of the bolometer by the background P_{IR} is important as described above, the first two terms in Eq.(5.2) are determined by this background. For a good bolometer readout, the responsivity should be large enough that the Johnson noise term is not dominant. As long as this condition is met, the heat capacity C of the bolometer is not a critical parameter. When the background power P_{IR} is small, then C should be as small as possible. The bolometer is then operated with $\omega\tau$=1 and G is chosen so that the phonon and Johnson noise terms are equal.

Bolometers for millimeter and submillimeter radiation generally use a composite structure with a 200 Ω/□ metal film absorber on a low heat capacity dielectric substrate such as diamond or sapphire [51]. One such bolometer used the transition edge in an Al film with R~10 Ω and T_c=1.3 K [51]. To avoid amplifier noise, this bolometer was ac biased at 1 KHz and transformer coupled to an FET amplifier. Low frequency feedback was used to maintain the operating point in the center of the resistive transition. The resulting NEP=1.7×10^{-15} $WHz^{-1/2}$ with a response time τ=83 ms, is comparable to, but not better than, composite bolometers with semiconducting thermometers operated at the same temperature [52] and much less sensitive than semiconducting bolometers operated at lower temperatures. Similar performance was obtained with bolometers which used SNS and SIN tunnel junction thermometers at 1.5 K and SQUID readouts [53]. None of these bolometers are used because they have similar performance to the semiconductor bolometers, but the electronic systems are more complicated.

The suggestion has been made recently [54] that a sensitive bolometer can be made by using a SQUID to measure the temperature dependent kinetic inductance [2] of a superconducting microstrip. The estimated loss in the microstrip is so low that the noise resulting from resistive dissipation [analogous to the Johnson noise term in Eq.(5.2)] can be neglected. Improved performance can then be obtained in the low P_{IR} (heat capacity dominated) limit by operating with $\omega\tau>>1$ so as to minimize G and the associated phonon noise. It was estimated that NEP can be as low as $7\times10^{-20}WHz^{-1/2}$. It appears that the kinetic inductance mode of operation will be useful for very low temperature (T~100 mK) X-ray bolometers which give output pulses proportional to the energy of the absorbed X-ray photons [55]. Transition edge bolometers are not useful in this application because the energy of a single X-ray photon exceeds the dynamic range of the bolometer at such low temperatures.

A design study has been carried out for a high T_c transition edge bolometer with T_c=90 K and T_o=80 K [56]. Assuming $A\Omega=10^{-2}srcm^2$, T_B=300 K and $\omega/2\pi$=10 Hz, a high T_c bolometer for use at all infrared wavelengths is heat capacity limited for values of C~1-10 μJ/K characteristic of 30 μm thick diamond or $SrTiO_3$ substrates, but could be P_{IR} heating limited for $C\sim10^{-1}$ μJ/K, which could be obtained with a submicron membrane substrate. Measurements suggest that 1/f noise in good quality c-axis YBCO films will not reduce bolometer performance significantly [56]. Values of NEP from $1-20\times10^{-12}WHz^{-1/2}$, predicted from this analysis, are small enough to compete with commercial room temperature and LN temperature infrared detectors for $\lambda>13$ μm.

Superconducting Photon Detectors

A current-biased superconducting film deposited directly onto a heat sink at T_c can be used as a fast transition edge bolometer for detecting pulses of photons or phonons. Early work on these bolometers gave evidence for two kinds of fast response in granular films, one of which was not thought to be bolometric. Recent interest in such phenomena was stimulated by detection experiments [57] on granular films of the oxide superconductor $BaPb_{0.7}Bi_{0.3}O_3$ which has $T_c \approx 12$ K. The film was patterned into a long thin meander strip, which was crossed by a large number N of grain boundaries. A responsivity of 10^4 V/W was observed for infrared wavelengths from 1-10 μm. Response was seen at frequencies beyond 1 GHz.

If this detector is modeled as a series array of N boundary Josephson junctions, the Josephson direct detector response expected at millimeter wavelengths will be very small at 1 μm wavelength because of the frequency dependence $(\omega_c/\omega_s)^2$. Bolometric response is also possible, but probably not at 1 GHz. The authors ascribed their observed response to pair breaking by the incident photons which can decrease the energy gap and change both the quasiparticle and the Josephson pair tunneling in the grain boundary junctions. They argued that by decreasing the width and increasing the length of the meander strip, the NEP should vary $N^{-1/2}$, reaching values as low as 10^{-13} $WHz^{-1/2}$ for a 10×10 μm^2 detector. Few detailed noise measurements were presented. To compare detectors with different areas the figure of merit $D^*=A^{1/2}/NEP$, called the specific detectivity, is often used. The predicted NEP corresponds to $D^* \approx 10^9$ $cmHz^{1/2}$ ω^{-1}.

Considerable excitement has been generated by the possibility that such detectors could be usefully implemented in high T_c films and operated at LN

temperatures. A theoretical estimate [58] based on the principle that a photon detector should have more photo-generated carriers than thermally generated carriers suggests, however, that a high T_c photon detector optimized for the detection of room temperature blackbody radiation would require a much lower operating temperature than the conventional HgCdTe photovoltaic detectors. A number of workers [59-61] are measuring the response of NbN, LaSrCuO, and YBCO films of many types to visible and infrared laser radiation. There is evidence for bolometric responses on more than one time scale that peak near T_c where dR/dT is large. A second type of response is observed near $T_c/2$ in granular films that is ascribed to phase slips [57,59,60] that occur because the excitation of quasiparticles reduces the Josephson critical current of the grain boundary junctions. The value of D^* reported in these experiments is usually below 10^8 $cmHz^{1/2}W^{-1}$, which is not large enough to be competitive in most applications. Experiments on optical detection by suppression of the gap voltage in Nb tunnel junctions are also being done [62].

Acknowledgments

The authors are grateful to C.A. Mears, A.D. Smith, and H.K. Olsson for many helpful discussions. This work was supported in part by the Director, Office of Energy Research, Office of Basic Energy Sciences, Materials Sciences Division of the U.S. Department of of Energy under Contract No. DE-AC03-76-SF00098, and by the Department of Defense.

[1] P.L. Richards and L.T. Greenberg, "Infrared Detectors for Low-Background Astronomy: Incoherent and Coherent Devices from One Micrometer to One Millimeter," Infrared and Millimeter Waves, vol. 6, pp. 149-207, 1982.

[2] T. Van Duzer and C.W. Turner, **Principles of Superconducting Devices and Circuits**, Elsevier North Holland, Inc., New York, 1981.

[3] A. Barone and G. Paterno, **Physics and Applications of the Josephson Effect**, John Wiley & Sons, New York, 1982.

[4] K.K. Likharev, **Dynamics of Josephson Functions and Circuits**, Gordon and Breach Science Publishers, New York, 1986.

[5] J.R. Tucker and M.J. Feldman, "Quantum Detection at Millimeter Wavelengths," Rev. Mod. Phys., vol. 57, No. 4, pp. 1055-1113, 1985.

[6] C.A. Mears, Qing Hu, and P.L. Richards, "Numerical Simulation on Experimental Data from Planar SIS Mixers with Integrated Tuning Elements," to be published in IEEE Trans. Magn., vol. MAG-25, 1989.

[7] A.V. Räisänen, D.G. Crété, P.L. Richards, and F.L. Lloyd, "A 100 GHz SIS Quasiparticle Mixer with 10 dB Coupled Gain," IEEE MTT-S Digest, pp. 929-930, 1987.

[8] J. Ibruegger, K. Okuyama, R. Blundell, K.H. Gundlach, and E.J. Blum, "Quasiparticle 150 GHz Mixer with a Submicron Pb/Bi/In-Oxide-Pb/Bi Junction," LT-17 (Contributed Papers), pp. 937-938, Elsevier Science Publishers, 1984.

[9] M.J. Feldman, "Quantum Noise in the Quantum Theory of Mixing," IEEE Trans. Magn. vol. MAG-23, No. 2, pp. 1054-1057, 1987.

[10] I.A. Devyatov, L.S. Kuzmin, K.K. Likharev, V.V. Migulin, and A.B. Zorin, "Quantum Statistical Theory of Microwave Detection Using Superconducting Tunnel Junctions," J. Appl. Phys., vol. 60, pp. 1808-1828, 1986.

[11] M.J. Wengler and M.F. Bocko, "Beating the Quantum Limit in SIS Mixers," to be published in IEEE Trans. Magn., vol. MAG-25, 1989.

[12] M.J. Wengler and D.P. Woody, "Quantum Noise in Heterodyne Detection," IEEE J. Quantum Electron., vol. QE-23, pp. 613-622, 1987.

[13] W.R. McGrath, P.L. Richards, D.W. Face, D.E. Prober, and F.L. Lloyd, "Accurate Experimental and Theoretical Comparisons Between Superconductor-Insulator-Superconductor Mixers Showing Weak and Strong Quantum Effects," J. Appl. Phys. vol. 63, pp. 2479-2491, 1988.

[14] S.-K. Pan, A.R. Kerr, M.J. Feldman, A.W. Kleinsasser, J. Stasiak, R.L. Sandstrom, and W.J. Gallagher, "An 85-116 GHz SIS Receiver Using Inductively Shunted Edge-Junctions," submitted to IEEE Trans. Microwave Theory Tech., 1988.

[15] T.-M. Shen, "Conversion Gain in Millimeter Wave Quasiparticle Heterodyne Mixers," IEEE J. Quantum Electron. vol. QE-17, No. 7, pp. 1151-1165, 1981.

[16] M.J. Wengler, D.P. Woody, R.E. Miller and T.G. Phillips, "A Low Noise Receiver for Submillimeter Astronomy," Proceedings of the SPIE, vol. 598, pp. 27-32, 1985.

[17] D.G. Crété, W.R. McGrath, P.L. Richards, and F.L. Lloyd, "Performance of Arrays of SIS Junctions in Heterodyne Mixers," IEEE Trans. Microwave Theory Tech., vol. MTT-35, pp. 435-440, 1987.

[18] J.H. Magerlein, "Specific Capacitance of Josephson Tunnel Junctions," IEEE Trans. Magn., vol. MAG-17, pp. 286-289, 1981.

[19] M. Gurvitch, M.A. Washington, and H.A. Huggins, "High Quality Refractory Josephson Tunnel Junctions Utilizing Thin Aluminum Layers," Appl. Phys. Lett., vol. 42, pp. 472-474, 1983.

[20] W.R. McGrath, A.V. Räisänen, and P.L. Richards, "Variable Temperature Loads for use in Accurate Noise Measurements of Cryogenically Cooled Microwave Amplifiers and Mixers," Int. J. Infrared and Millimeter Waves, vol. 7, pp. 543-553, 1986.

[21] T.G. Phillips and D.P. Woody, "Millimeter- and Submillimeter- Wave Receivers," Ann. Rev. Astron. Astrophys. vol. 20, pp. 285-321, 1982.

[22] T.H. Büttgenbach, R.E. Miller, M.J. Wengler, D.M. Watson, and T.G. Phillips, "A Broadband Low Noise SIS Receiver for Submillimeter Astronomy," submitted to IEEE Trans. Microwave Theory Tech., 1988.

[23] R. Blundell, M. Carter, and K.H. Gundlach, "A Low Noise SIS Receiver Covering the Frequency Range 215-250 GHz," submitted to Int. J. Infrared and Millimeter Waves, Feb. 1988.

[24] P.T. Timbie and D.T. Wilkinson, "Low-Noise Interferometer for Microwave Radiometry," Rev. Sci. Instrum., vol. 59, pp. 914-920, 1988.

[25] M.W. Pospieszalski, S. Weinreb, R.D. Norrod, and R. Harris, "FET's and HEMT's at Cryogenic Temperatures--Their Properties and use in Low-Noise Amplifiers," IEEE Trans. Microwave Theory Tech., vol. MTT-36, pp. 552-560, 1988.

[26] L.R. D'Addario, "An SIS Mixer for 90-120 GHz with Gain and Wide Bandwidth," Int. J. Infrared and Millimeter Waves, vol. 5, No. 11, pp. 1419-1442, 1984.

[27] A.V. Räisänen, D.G. Crété, P.L. Richards, and F.L. Lloyd, "Wide-Band Low Noise MM Wave SIS Mixers with a Single Tuning Element," Int. J. Infrared and Millimeter Waves, vol. 7, pp. 1835-1851, 1986.

[28] A.R. Kerr, S.-K. Pan, and M.J. Feldman, "Integrated Tuning Elements for SIS Mixers," Int. J. Infrared and Millimeter Waves, vol. 9, No. 2, pp. 203-212, 1988.

[29] D.P. Woody, R.E. Miller, and M.J. Wengler, "85 to 115 GHz Receivers for Radio Astronomy," IEEE Trans. Microwave Theory Tech. vol. MTT-33, pp. 90-95, 1985.

[30] E.C. Sutton, private communication, 1988.

[31] R. Blundell and K.H. Gundlach, "A Quasiparticle SIN Mixer for the 230 GHz Frequency Range," Int. J. Infrared and Millimeter Waves, vol. 8, pp. 1573-1579, 1987.

[32] Li Xizhi, P.L. Richards, and F.L. Lloyd, "SIS Quasiparticle Mixers with Bow-Tie Antennas," Int. J. Infrared and Millimeter Waves, vol. 9, pp. 101-133, 1988.

[33] Qing Hu, C.A. Mears, P.L. Richards, and F.L. Lloyd, "Mm Wave Quasioptical SIS Mixers," to be published in IEEE Trans. Magn. vol. MAG-25, 1989.

[34] Qing Hu, C.A. Mears, P.L. Richards, and F.L. Lloyd, "Measurement of Integrated Tuning Elements for SIS Mixers with a Fourier Transform Spectrometer," Int. J. Infrared and Millimeter Waves, vol. 9, pp. 303-320, 1988.

[35] M.J. Feldman and L.R. D'Addario, "Saturation of the SIS Direct Detector and the SIS Mixer," IEEE Trans. Magn. vol. MAG-23, pp. 1254-1258, 1987.

[36] P.L. Richards, T.-M. Shen, R.E. Harris, and F.L. Lloyd, "Superconductor-Insulator- Superconductor Quasiparticle Junctions as Microwave Photon Detectors," Appl. Phys. Lett. vol. 36, pp. 480-482, 1980.

[37] P.L. Richards, "A Novel Superconducting Radiometer," (1989 to be published).

[38] P.L. Richards, "The Josephson Junction as a Detector of Microwave and Far Infrared Radiation," **Semiconductors and Semimetals**, vol. 12, pp. 395-439, R.K. Willardson and A.C. Beer, Eds., New York Academic Press, 1977.

[39] Y. Taur, J.H. Claassen, and P.L. Richards, "Conversion Gain in a Josephson Effect Mixer," Appl. Phys. Lett. vol. 24, pp. 101-103, 1974.

[40] Y. Taur, "Josephson-Junction Mixer Analysis Using Frequency-Conversion and Noise-Correlation Matrices," IEEE Trans. Electron Devices vol. ED-27, pp. 1921-1928, 1980.

[41] Y. Taur and A.R. Kerr, "Low-Noise Josephson Mixers at 45 GHz Using Recyclable Point Contacts," Appl. Phys. Lett., vol. 32, pp. 775-777, 1978.

[42] J.H. Claassen and P.L. Richards, "Point-Contact Josephson Mixers at 130 GHz," J. Appl. Phys., vol. 49, pp. 4130-4140, 1978.

[43] T.G. Blaney, "Josephson Mixers at Submillimeter Wavelengths: Present Experimental Status and Future Developments," in **Future Trends in Superconductive Electronics**, B.S. Deaver, Jr. et al., Eds., New York, AIP Conf. Proc. vol. 44, pp. 230-238, 1978.

[44] A.K. Jain, K.K. Likharev, J.E. Lukens, and J.E. Sauvageau, "Mutual Phase-Locking in Josephson Junction Arrays," Phys. Report, vol. 109, pp. 309-426, North-Holland, Amsterdam, 1984.

[45] R.P. Robertazzi and R.A. Buhrman, "Josephson Terahertz Local Oscillator," to be published in IEEE Trans. Magn. vol. MAG-25, 1989.

[46] J.E. Lukens, A.K. Jain, and K.L. Wan, "Application of Josephson Effect Arrays for Submillimeter Sources," presented at NATO Advanced Study Institute on Superconducting Electronics, 1988.

[47] T. Nagatsuma, K. Enpuku, F. Irie, and K. Yoshida, "Flux-Flow Type Josephson Oscillator for Millimeter and Submillimeter Wave Region," J. Appl. Phys., vol. 54, pp. 3302-3309, 1983.

[48] A.D. Smith, R.D. Sandell, J.F. Burch, and A.H. Silver, "Low Noise Microwave Parametric Amplifier," IEEE Trans. Magn., vol. MAG-21, pp. 1022-1028, 1985.

[49] H.K. Olsson and T. Claeson, "Low Noise Josephson Parametric Amplification and Oscillations at 9 GHz," to be published in J. Appl. Phys., 1988.

[50] B. Yurke, P.G. Kaminsky, R.E. Miller, E.A. Shittaker, A.D. Smith, A.H. Silver, and R.W. Simon, "Observation of 4.2-K Equilibrium-Noise Squeezing via a Josephson-Parametric Amplifier," Phys. Rev. Lett., vol. 60, pp. 764-767, 1988.

[51] J. Clarke, G.I. Hoffer, P.L. Richards, and N.-H. Yeh, "Superconductive Bolometers for Submillimeter Wavelengths," J. Appl. Phys. vol. 48, pp. 4865-4879, 1977.

[52] A.E. Lange, E. Kreysa, S.E. McBride, and P.L. Richards, "Improved Fabrication Techniques for Infrared Bolometers," Int. J. Infrared and Mm Waves, vol. 4, pp. 689-706, 1983.

[53] J. Clarke, G.I. Hoffer, and P.L. Richards, "Superconducting Tunnel Junction Bolometers," Revue de Physique Appliquée, pp. 69-71, 1974.

[54] D.G. McDonald, "Novel Superconducting Thermometer for Bolometric Applications," Appl. Phys. Lett. vol. 50, pp. 775-777, 1987.

[55] S.E. Labov, private communication, 1988.

[56] P.L. Richards, J. Clarke, R. Leoni, Ph. Lerch, and S. Verghese, "Feasibility of the High T_c Superconducting Bolometer," submitted to Appl. Phys. Lett. 1988.

[57] Y. Enomoto and T. Murakami, "Optical Detector Using Superconducting $BaPb_{0.7}Bi_{0.3}O_3$ Thin Films," J. Appl. Phys., vol. 59, pp. 3807-3814, 1986.

[58] M. Kinch, private communication, 1988.

[59] M. Leung, U. Strom, J.C. Culbertson, J.H. Claassen, S.A. Wolf, and R.W. Simon, "NbN/BN Granular Films--A Sensitive, High-Speed Detector for Pulsed Far-Infrared Radiation," Appl. Phys. Lett. vol. 50, pp. 1691-1693, 1987.

[60] M. Leung, P.R. Broussard, J.H. Claassen, M. Osofsky, S.A. Wolf, and U. Strom, Appl. Phys. Lett. vol. 51, pp. 2046-2047, 1987.

[61] M.G. Forrester, M. Gottlieb, J.R. Gavaler, and A.I. Braginski, "Optical Response of Epitaxial Films of $YBa_2Cu_3O_{7-\delta}$," to be published in Appl. Phys. Lett. 1988.

[62] D.P. Osterman, R. Drake, R. Patt, E.K. Track, M. Radparuar, and S.M. Faris, "Optical Response of YBCO Thin Films and Weak-Links," to be publisehd in IEEE Trans. Magn. vol. MAG-25, 1989.

FIGURE CAPTIONS

Fig. 1. Line (a) is the experimental I-V curve for a Nb/Pb-alloy SIS junction at $T<<T_c$ traced in the direction of decreasing current. The Josephson current at zero voltage seen when the I-V curve is traced in the direction of increasing current is not shown.
Dotted line (b) is the same I-V curve pumped at 90 GHz with an LO source whose admittance is high compared with R_N^{-1} (constant voltage source).
Solid line (b) is the photon assisted tunneling calculated from the DC I-V curve and Eq.(2.2)
Dotted line (c) is the same junction pumped from a 90 GHz LO source whose admittance is small compared with R_N^{-1}.
Solid line (c) is the photon assisted tunneling calculated from the quantum theory of mixing with the admittance at the LO port adjusted for the best fit [6].

Fig. 2. Functional circuit for a mixer made using a nonlinear diode pumped at ω_{LO}. The imbedding admittances of the mixer at frequencies $\omega_m=m\omega_{LO}+\omega_0$, where $\omega_0=\omega_{IF}$, $\omega_1=\omega_S$ and $\omega_{-1}=\omega_I$, are given by Y_m. There is a small signal applied at $\omega_1=\omega_S$. Noise can drive the mixer at other frequencies.

Fig. 3. Curves describing the performance of an SIS quasiparticle mixer [8]. The line labeled 1 is the unpumped I-V curve. Line 2 is the I-V curve when pumped with a LO at 150 GHz. Line a is the IF output power with a 300 K load at the input and line b is the output power for a 77 K load. The mixer is

unstable for bias V<2.2 mV because of Josephson effects. Measured values of $T_{R(DSB)}$ were 102 K on the first photon peak and 81 K on the second photon peak below $2\Delta/e$.

Fig. 4. Cross section of a W-band SIS quasiparticle mixer with two mechanical adjustments for RF matching [14]. The SIS junction with a lithographed RF matching structure is deposited on a Si chip that is bonded to the suspended stripline used to provide dc bias and IF output.

Fig. 5. A summary of some of the best results for the single sideband noise temperature of SIS quasiparticle and Schottky diode heterodyne receivers [22].

Fig. 6. Scalar feed horn and mixer block used for an SIS quasiparticle mixer from 85 to 115 GHz [29]. This mixer uses circular waveguide and a single mechanical tuning element for RF matching.

Fig. 7. Cross section of the optical system used with a planar lithographed SIS quasiparticle mixer [16]. The junction and antenna are located on a quartz substrate attached to the back surface of a quartz lens.

Fig. 8. Layout of window junctions and lithographed RF matching structures used in quasioptical SIS quasiparticle mixers from 90 to 270 GHz [33].
Diagram a) shows a series array of five junctions with a parallel wire inductor terminated in an open-ended $\lambda/4$ microstrip stub.
b) Shows a single junction with an inductive open-ended $3\lambda/8$ stub.
c) Shows a single junction with an inductive $\lambda/8$ stub whose end is RF shorted by an open-ended $\lambda/4$ stub.

Fig. 9. (a) I-V curve of an Nb point-contact junction. The load line used for the direct detector is indicated.
(b) The same junction with sufficient P_{LO} to reduce the zero-voltage current to $I_c/2$. The load line used for the heterodyne mixer is indicated.
(c) Mixer output as a function of bias voltage showing peaks at voltages where R_D is large [39].

Fig. 10. Layout of a Josephson effect oscillator for ~360 GHz [46] described in the text. The 40 phase-locked junctions are connected in series at RF, but are individually biased with the same static voltage V.

Fig. 11. Equivalent circuit for a Josephson parametric amplifier. The junction is represented by its nonlinear Josephson inductance L_J, quasiparticle resistance R, and capacitance C. An external inductor L is added to resonate the junction capacitance at ω_S. When pumped, the combined impedance Z_J can be negative, causing gain in the reflected signal power.

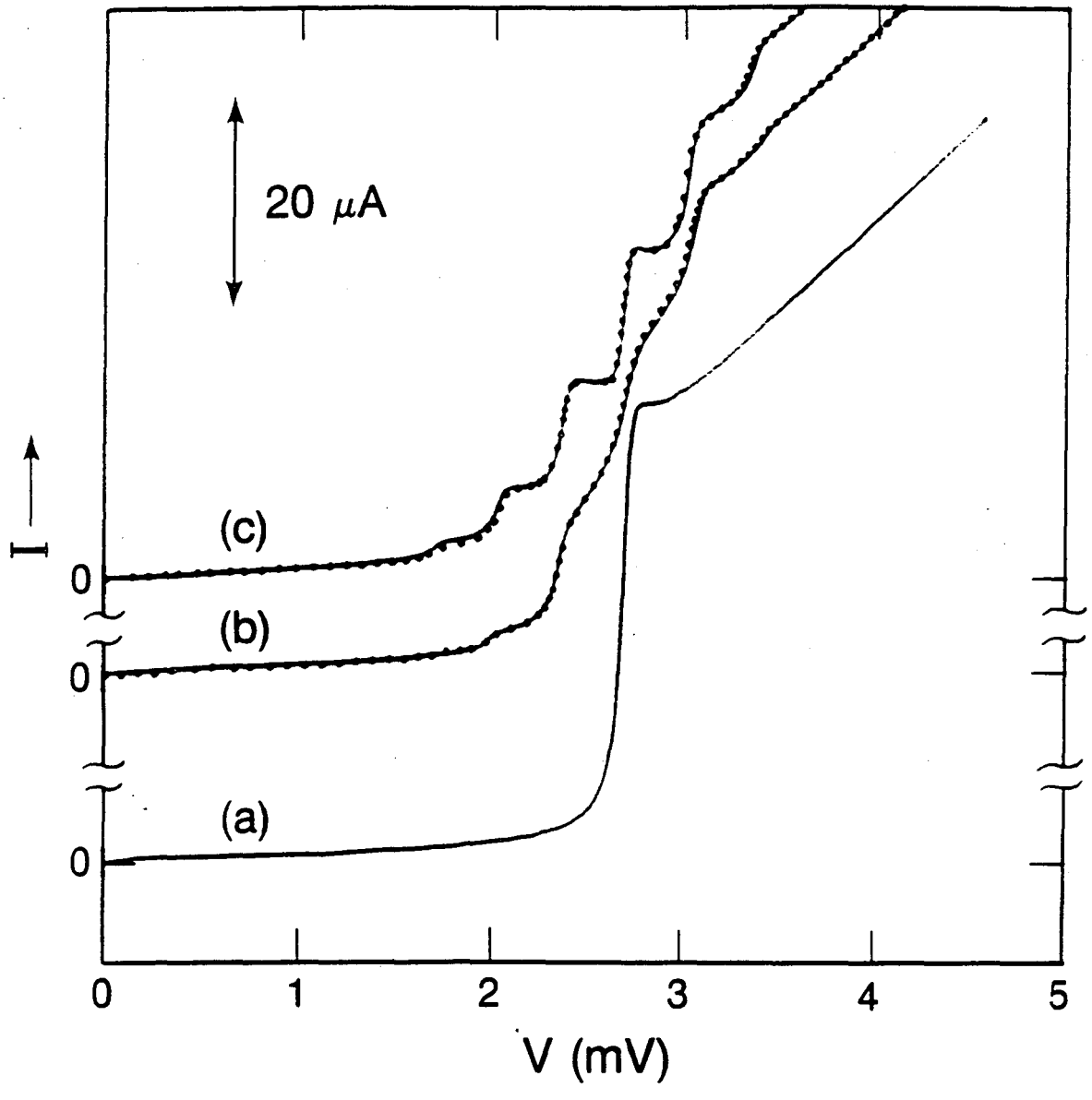

XBL 8810-7612

FIGURE 1

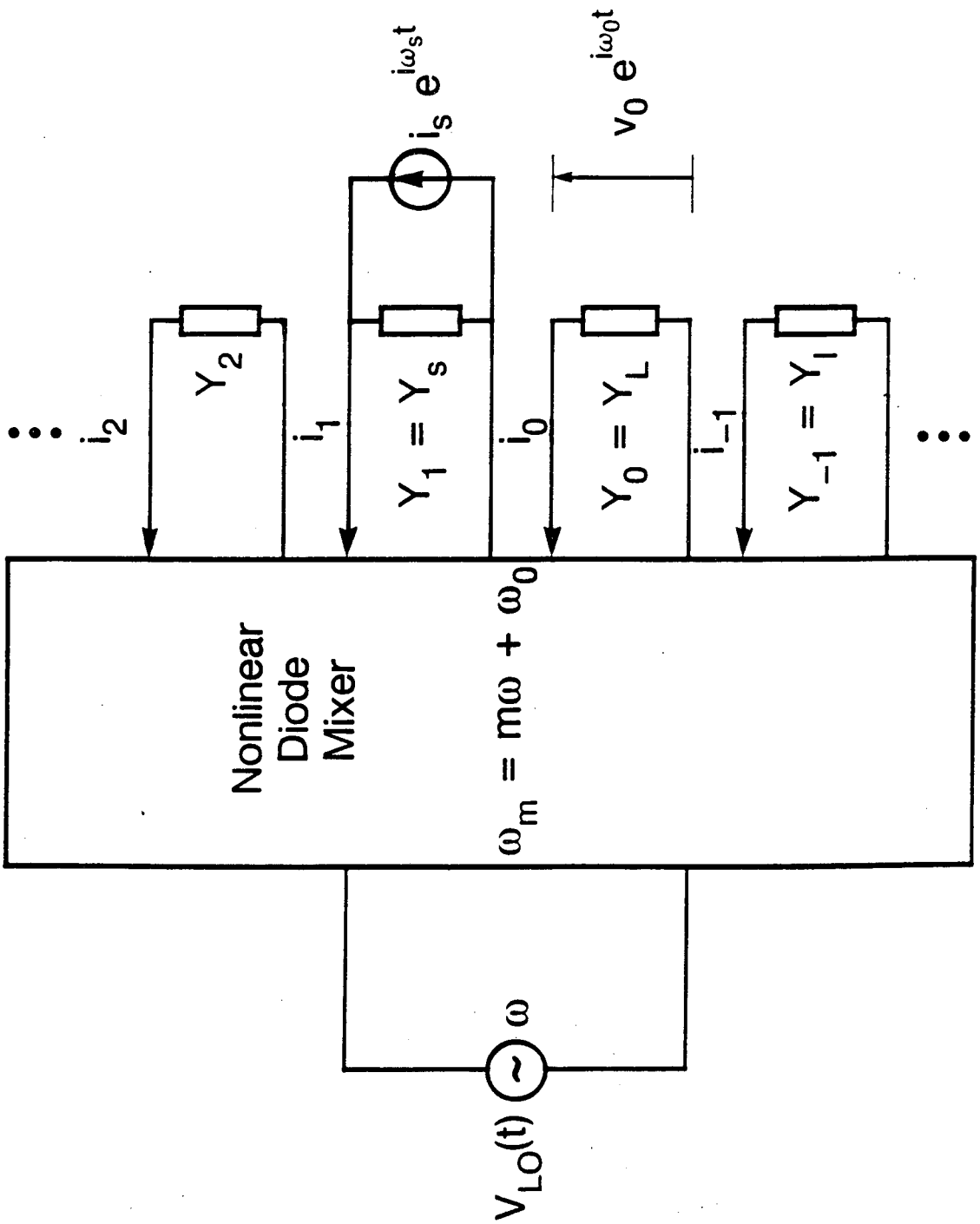

XBL 8810-7609

FIGURE 2

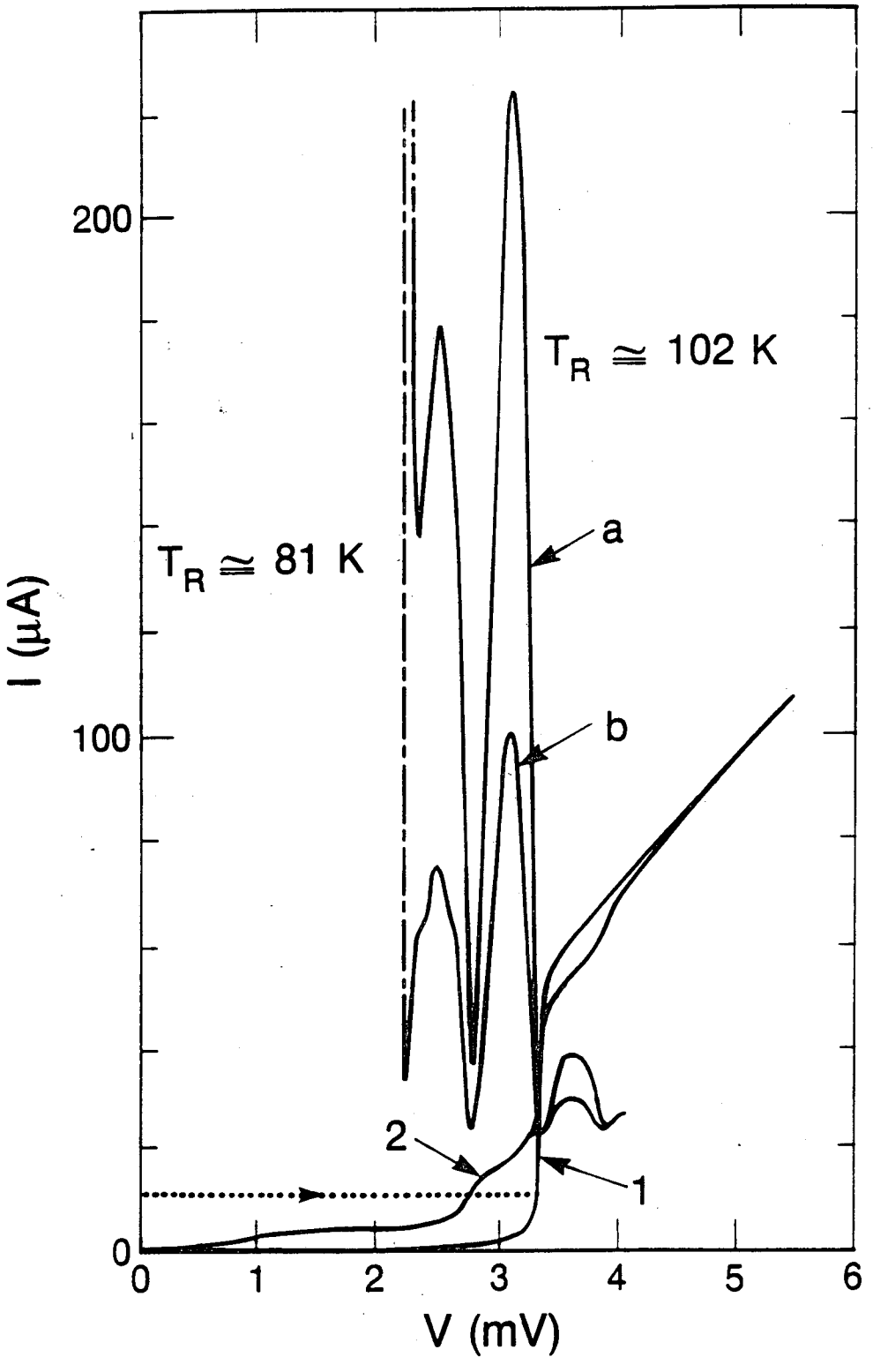

XBL 8810-7604

FIGURE 3

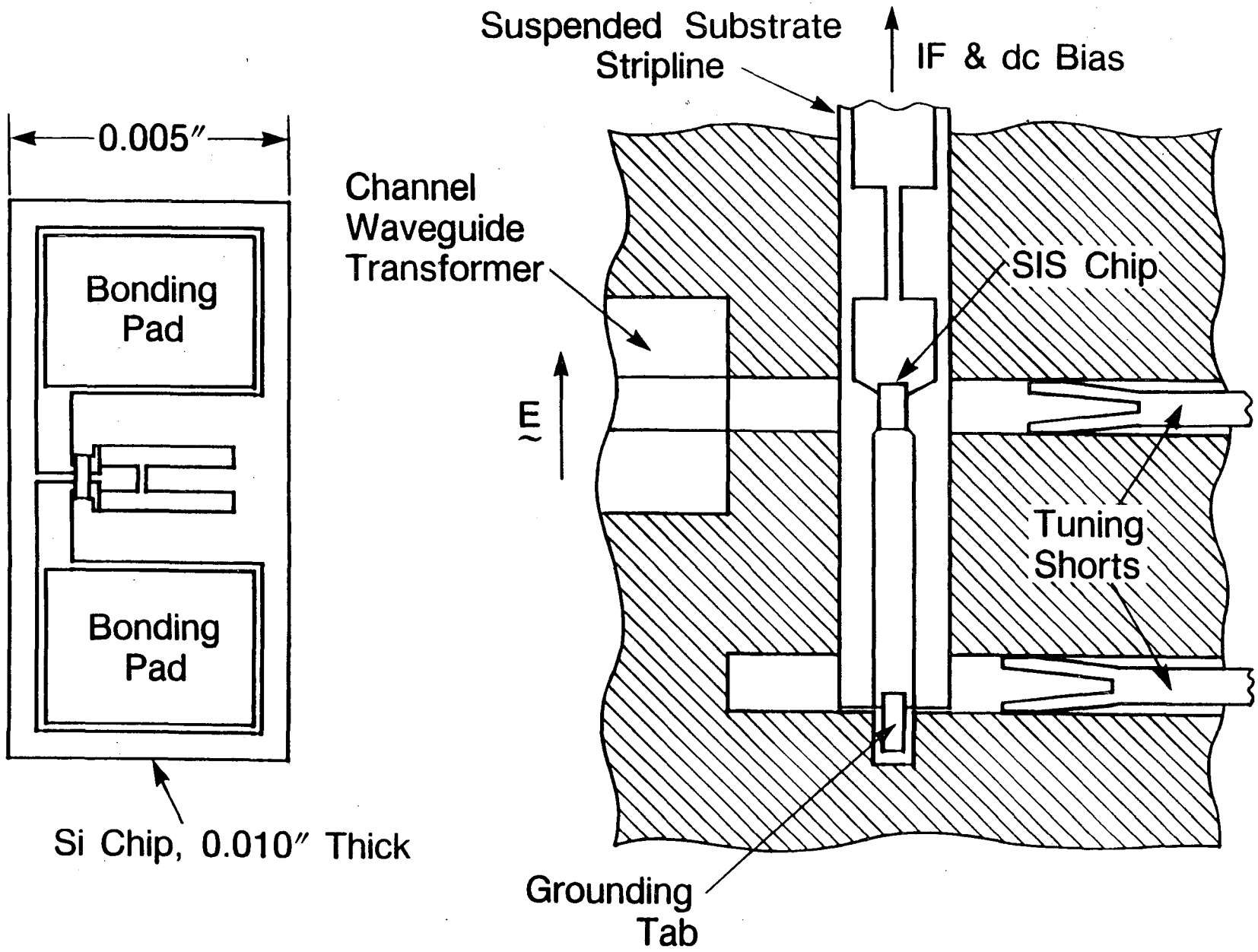

FIGURE 4

XBL 8810-7608

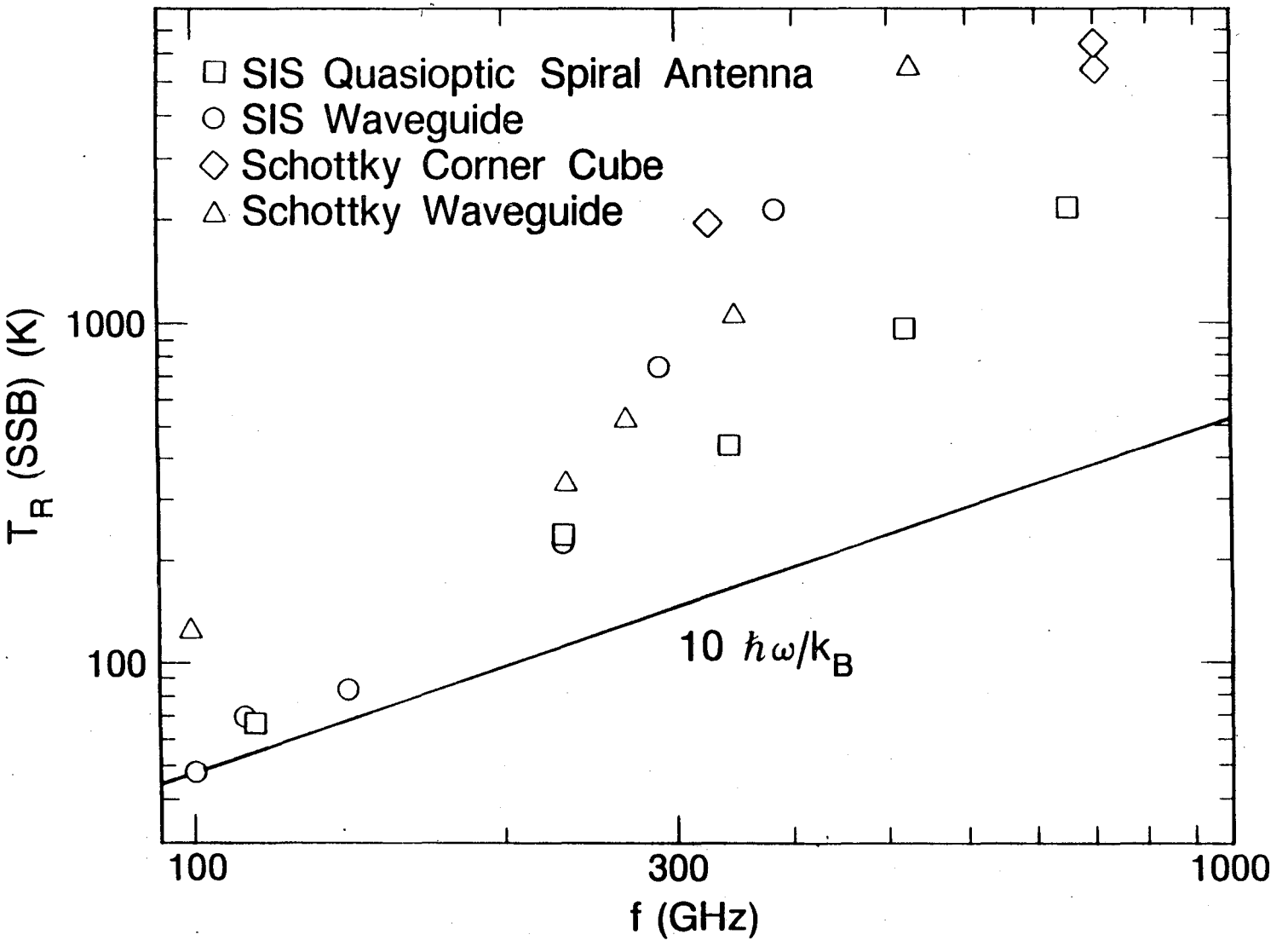

FIGURE 5

XBL 8810-7610

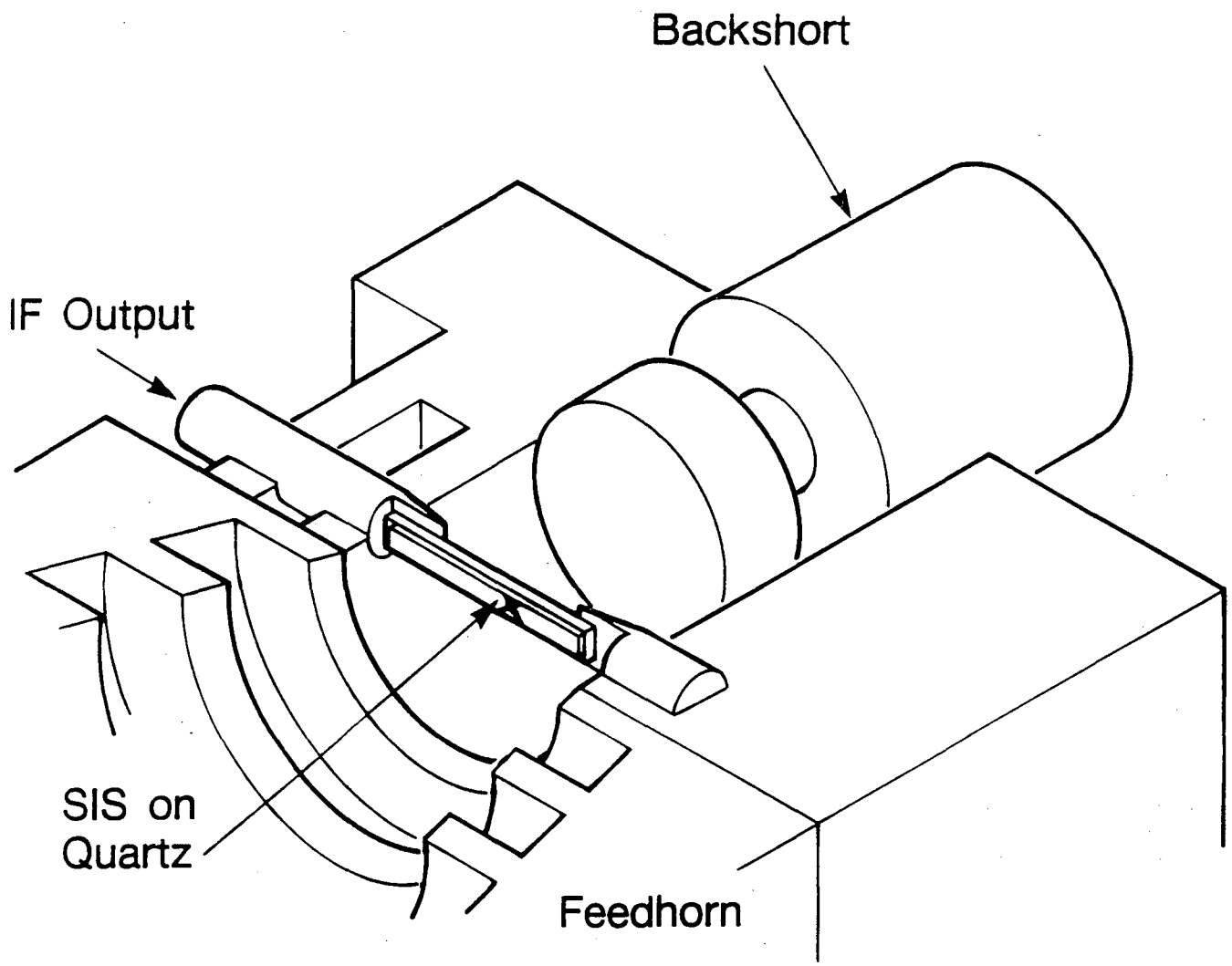

XBL 8810-7607

FIGURE 6

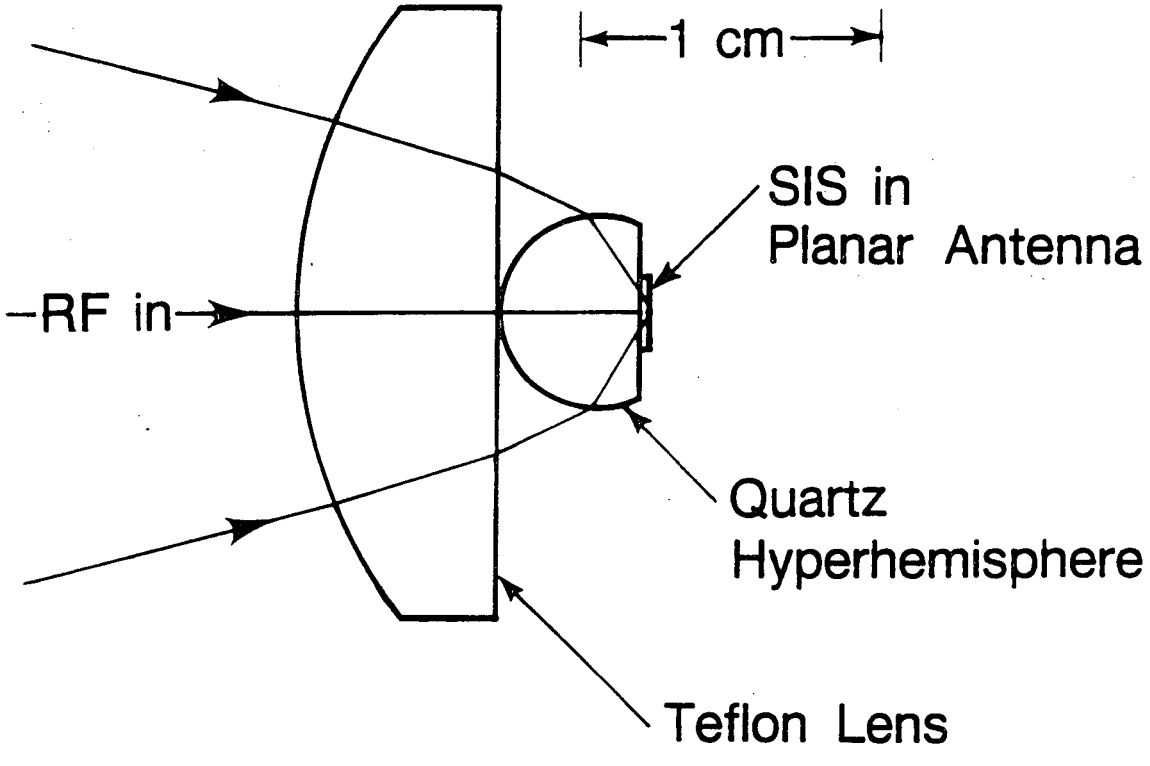

XBL 8810-7611

FIGURE 7

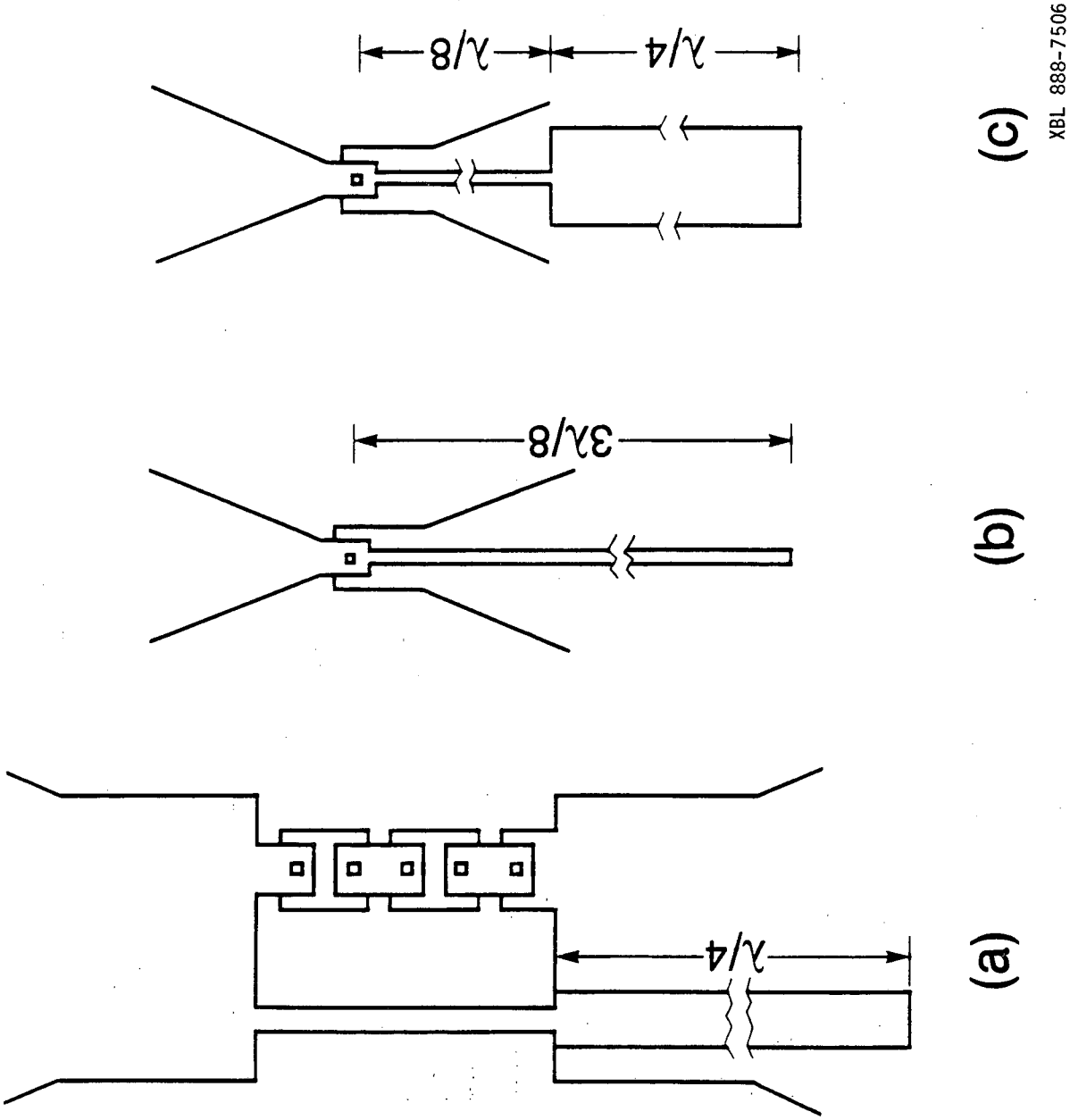

XBL 888-7506

FIGURE 8

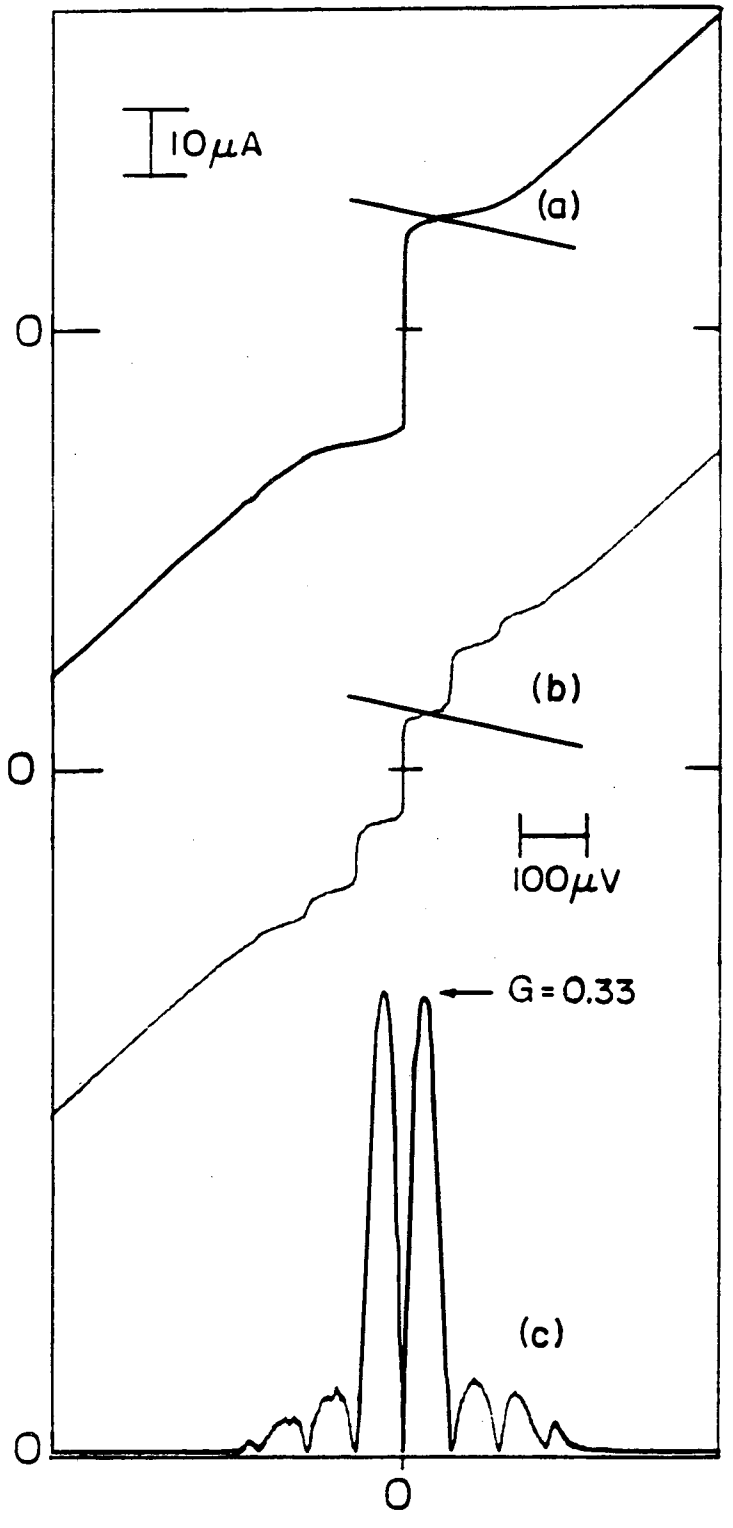

XBL 737-6554B

FIGURE 9

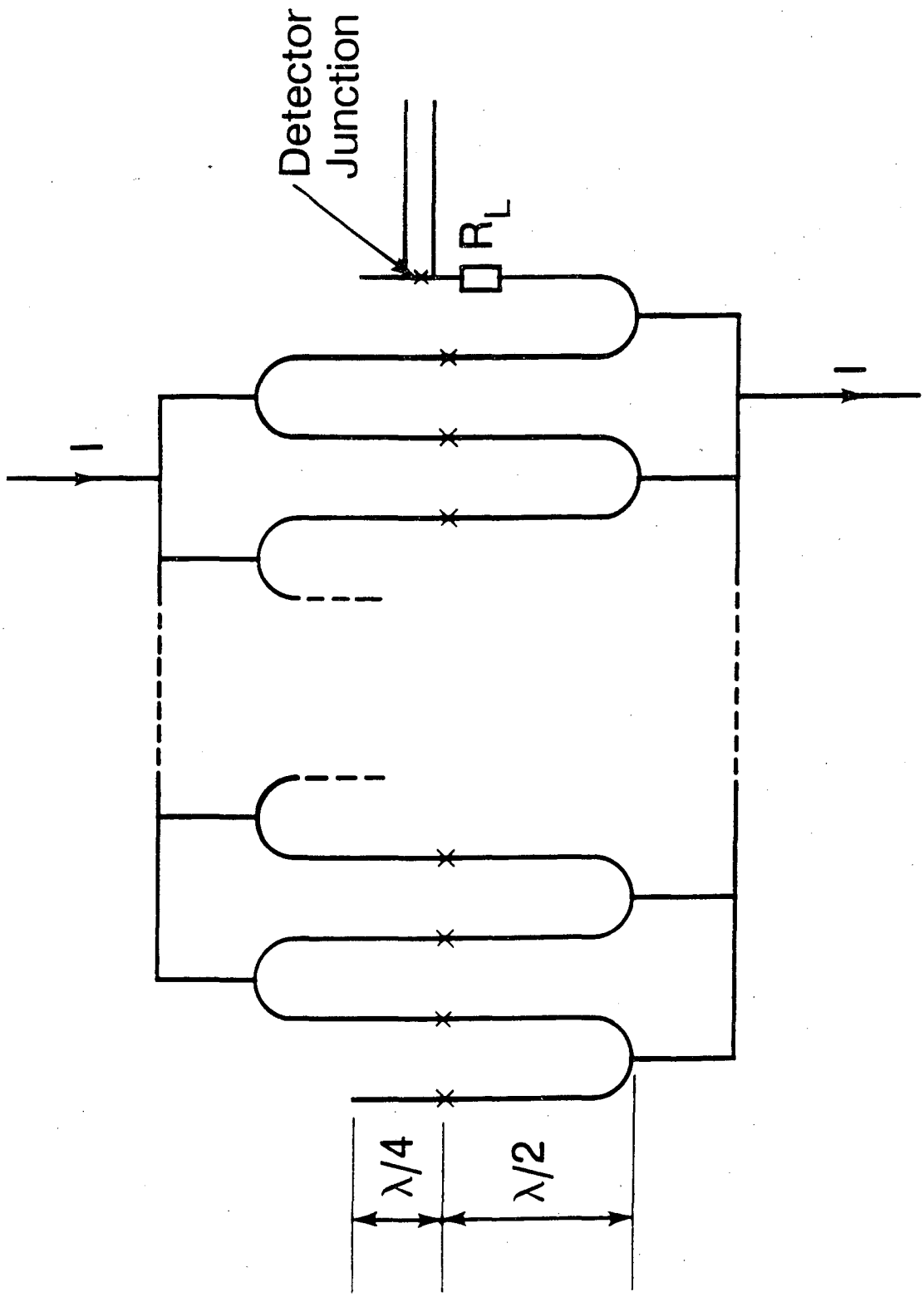

XBL 8810-7620

FIGURE 10

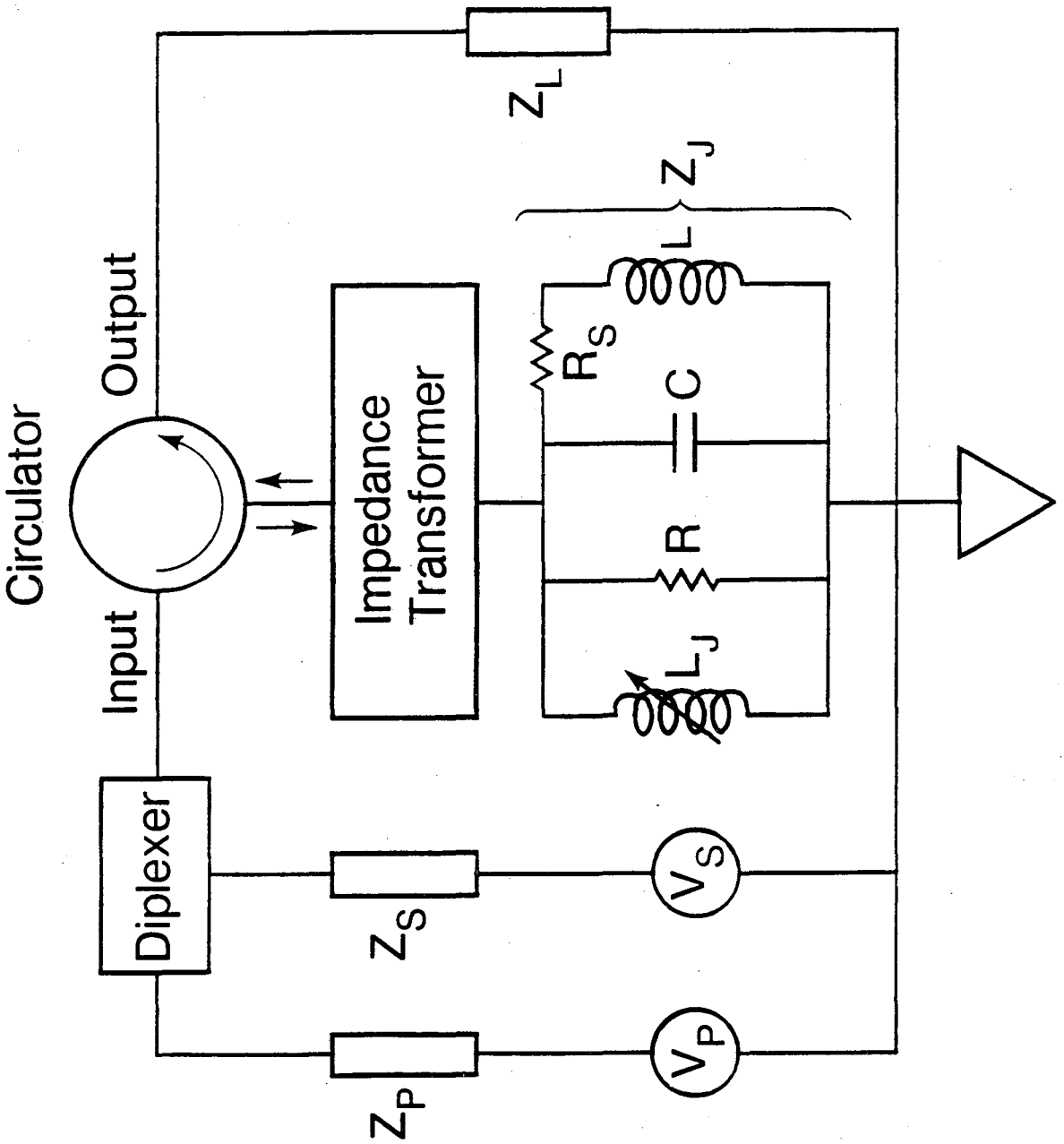

XBL 8810 7621

FIGURE 11

LAWRENCE BERKELEY LABORATORY
CENTER FOR ADVANCED MATERIALS
1 CYCLOTRON ROAD
BERKELEY, CALIFORNIA 94720